**T.C.**
**MARMARA UNIVERSITY**
**INSTITUTE FOR GRADUATE STUDIES IN**
**PURE AND APPLIED SCIENCES**

# MATHEMATICAL MODEL BASED OPTIMIZATION OF A PACKED BED HEAT STORAGE TANK

**Osman ÖZDEMİR**

**THESIS**
**FOR THE DEGREE OF MASTER OF SCIENCE**
**IN**
**CHEMICAL ENGINEERING PROGRAMME**

**SUPERVISOR**
**Assoc. Prof. Dr. Kurtul KÜÇÜKADA**

**ISTANBUL 2011**

**T.C.**
**MARMARA UNIVERSITY**
**INSTITUTE FOR GRADUATE STUDIES IN**
**PURE AND APPLIED SCIENCES**

# MATHEMATICAL MODEL BASED OPTIMIZATION OF A PACKED BED HEAT STORAGE TANK

**Osman ÖZDEMİR**
(524509005)

**THESIS**
**FOR THE DEGREE OF MASTER OF SCIENCE**
**IN**
**CHEMICAL ENGINEERING PROGRAMME**

**SUPERVISOR**
**Assoc. Prof. Dr. Kurtul KÜÇÜKADA**

**ISTANBUL 2011**

# ACKNOWLEDGEMENT

I see this work as a triumph of enthusiasm and good planning and discipline. Studying efficiently, without wasting any time or information and accuracy while surveying the literature were the keys to get this thesis accomplished, successfully.

In the first place, I would like to record my gratitude to Assoc. Prof. Dr. Kurtul KÜÇÜKADA for his supervision, advice and guidance from the very early stage of this thesis as well as giving me his extraordinary experiences and insights.

I gratefully acknowledge the previous studies made in our department; they made it possible, gathering such an experimental setup to be used for this thesis. I am also grateful to all of the members of Chemical Engineering Department in Marmara University, especially, Assoc. Prof. Dr. Perviz SAYAN.

Above all, I wish to express my love and gratitude to all my family who have always supported me. Also, I wish to dedicate this work to my beloved parents Hülya and Yücel.

Last but not the least; I want to express my gratitude to Prof. Dr. Neşet KADIRGAN and Assist. Prof. Dr. Emre ALPMAN for their valuable comments and questions during my presentation.

12.07.2011

Osman ÖZDEMİR

# CONTENTS

# ABSTRACT

## MATHEMATICAL MODEL BASED OPTIMIZATION OF A PACKED BED HEAT STORAGE TANK

In this work, temperature distribution profile of a packed bed heat storage (PBHS) unit was investigated for developing a mathematical model and optimizing the tank, where, the heat transfer mechanisms were conduction, advection, convection and natural convection, and packing material was glass beads.

The suggested mathematical model was analyzed in the aspects of the made assumptions, the physical properties of fluid and solid, effect of thermal mixing, advection and forced convection, the model parameters and the bed properties. Especially, a thermal mixing phenomenon which was observed during heating cycles was taken as the primary focus in most investigations. **Unfortunately, there is no related work published in the literature analyzing and bringing a clear understanding to the thermal mixing phenomena due to buoyancy forces resulting from the temperature difference between the inlet and the outlet of the PBHS unit**.

In all experiments, fluid inlet temperature and fluid flow rate thus the fluid velocity were taken as the manipulated variables to check the effects of the thermal dispersion coefficient $k_d$ and the convective heat transfer coefficient $h$ on the experimental results. The experiments were performed as cooling and heating experiments depending on the inlet fluid temperature and the initial temperature of the packed bed. All of the obtained experimental results were compared to the results obtained by using the model. The significant and relevant aspects of the experimental results were considered and discussed with conjunction to the behavior of the model.

Using the developed mathematical model, minimum heat storage time, maximum heat storage capacity and optimum flow rate of the PBHS unit was suggested as dimensionless time to optimize the system.

**Key Words:** Packed bed, mathematical modeling, thermal dispersion, heat storage, advection, and optimization.

**July 2011** **Osman ÖZDEMİR**

# ÖZET

## DOLGULU YATAKLI ISI DEPOSUNUN MATEMATİKSEL MODEL DESTEKLİ OPTİMİZASYONU

Isı transferi mekanizmalarının iletim, adveksiyon konveksiyon ve doğal konveksiyon olduğu ve dolgu maddesi olarak cam bilyelerin kullanıldığı bu çalışmada, dolgulu yataklı ısı deposu (DYID) ünitesinin matematiksel modellenmesi ve optimize edilmesi amacıyla tanktaki sıcaklık dağılımı profilleri incelenmiştir.

Önerilen matematiksel model, sıvının ve katının fiziksel özellikleri ve termal dispersiyonun, adveksiyonun, konveksiyonun, model parametrelerinin ve yatak özelliklerinin etkileri açısından analiz edilmiştir. Yapılan incelemelerin çoğunda, özellikle ısıtma döngülerinde görülen termal dispersiyon olayına odaklanılmıştır. **Ne yazık ki, DYID ünitesinin giriş ve çıkış sıcaklıkları arasındaki fark dolayısıyla meydana gelen kaldırma kuvvetlerinin (Buoyancy Forces) etkisi ile oluşan termal dispersiyon olayına net bir açıklama getiren veya analiz eden bilimsel bir yayının varlığına rastlanmamıştır.**

Tüm deneylerde, deney sonuçları üzerine termal dispersiyon katsayısının $k_d$ ve konveksiyonel ısı transferi katsayısının $h$ etkilerini kontrol etmek amacıyla, sıvı giriş sıcaklığı ve sıvı giriş debisi değiştirilmiştir. Deneyler, sıvı giriş sıcaklığı ve yatağın başlangıç sıcaklığına göre ısıtma ve soğutma döngüleri olarak yapılmıştır. Aynı koşullar deneylerden elde edilen tüm sonuçlar, model sonuçları ile karşılaştırılmıştır. Deneysel sonuçların tüm önemli ve ilgili kısımları, geliştirilen matematiksel model açısından incelenmiş ve tartışılmıştır.

Geliştirilen matematiksel modeli kullanarak DYID ünitesinin minimum ısı depolama süresi, maksimum ısı depolama kapasitesi ve optimum debisi sitemi optimize edebilmek amacıyla boyutsuz zaman cinsinden önerilmiştir.

**Anahtar Kelimeler:** Dolgulu yatak, matematiksel modelleme, termal dispersiyon, ısı deposu, adveksiyon ve optimizasyon.

**Temmuz 2011** **Osman ÖZDEMİR**

# LIST OF SYMBOLS

$\boldsymbol{A}$ : Heat transfer area ($m^2$)

$\boldsymbol{a}$ : Specific surface area of glass beads $6(1-\varepsilon)/D_p$ ($m^2/m^3$)

$\boldsymbol{a_t}$ : Specific heat transfer surface ($S_t/V_t$) ($m^2/m^3$)

$\boldsymbol{C}$ : Heat capacity (J/kg ºC)

$\boldsymbol{C_f}$ : Heat capacity of fluid (J/kg ºC)

$\boldsymbol{D_p}$ : Particle diameter (m)

$\boldsymbol{D_{tank}}$ : Tank diameter (m)

$\boldsymbol{g}$ : Gravity ($m/s^2$)

$\boldsymbol{h}$ : Convective heat transfer coefficient of the packed bed ($J/m^2$ s ºC)

$\boldsymbol{K}$ : Permeability of the packed bed $((\varepsilon^3 D_p^2)/(180(1-\varepsilon)^2))$

$\boldsymbol{k}$ : Thermal conductivity of fluid (J/m s ºC)

$\boldsymbol{k_m}$ : Thermal conductivity of material (J/m s ºC)

$\boldsymbol{k_d}$ : Axial thermal dispersion coefficient of fluid (J/m s ºC)

$\boldsymbol{k_{tank}}$ : Thermal conductivity of the tank (J/m s ºC)

$\boldsymbol{L}$ : Bed length (m)

$\boldsymbol{q}$ : Heat transfer rate (J/s)

$\boldsymbol{S_t}$ : Empty tank surface ($m^2$)

$\boldsymbol{T}$ : Working fluid temperature (ºC)

$\boldsymbol{T_s}$ : Packing material temperature (ºC)

$\boldsymbol{t}$ : Time (s)

$\boldsymbol{T_0}$ : Initial temperature (ºC)

$\boldsymbol{T_\infty}$ : Infinite temperature (ºC)

$\boldsymbol{U}$ : Overall heat transfer coefficient ($J/m^2$ºC)

$\boldsymbol{V_{flow}}$ : Working fluid flow rate (L/s)

$\boldsymbol{V_t}$ : Empty tank volume ($m^3$)

$\boldsymbol{V_z}$ : Fluid velocity (m/s)

**Greek Letters**

$\boldsymbol{\varepsilon}$ : Void fraction of packed bed ($V\varepsilon/V_{tank}$) ($m^3/m^3$)

$\boldsymbol{\alpha_m}$ : Media thermal diffusivity ($\alpha_m=k/(\rho C_f)$)

$\boldsymbol{\beta}$ : Thermal expansion (1/ ºC)

$\boldsymbol{\theta}$ : Dimensionless temperature

$\boldsymbol{\mu}$ : Dynamic viscosity of fluid (kg/m s)

$\boldsymbol{\nu}$ : Kinematic viscosity of fluid ($m^2/s$)

$\boldsymbol{\rho}$ : Density of fluid($kg/m^3$)

$\boldsymbol{\tau}$ : Dimensionless time

**Dimensionless Groups**

***Re*** : Reynolds number ($\rho_f D_p V z/\varepsilon\mu$)

***Pr*** : Prandtl number ($C_f\mu/k$)

***Nu*** : Nusselt number ($hD_p/k$)

***Pe*** : Peclet number (Re.Pr) ($\rho_f D_p V z C_f/\varepsilon k$)

***Gr*** : Grashof number ($g\beta\Delta T D^3/\nu$)

***Ra*** : Rayleigh number (Gr.Pr)

# ABBREVIATIONS

**PBHS** **:** Packed Bed Heat Storage

**Nu** **:** Nusselt Number

**Re** **:** Reynolds Number

**Pr** **:** Prandtl Number

**Pe** **:** Peclet Number

**2DADPF** **:** Two Dimensional Axial Dispersion Plug Flow

**GPCC** **:** Granular Phase Change Composites

**LHTES** : Latent Heat Thermal Energy Storage

**TESS** : Thermal energy storage system

**SHM** : Sensible heat Material

**PCM** : Phase change material

**Temp**. : Temperature

# LIST OF FIGURES

**PAGE NO**

# LIST OF TABLES

# CHAPTER I

## INTRODUCTION and AIM

### I.1 INTRODUCTION

Packed bed heat storage (PBHS) systems are extensively used in the chemical and process industries as reactors, separators, dryers, filters and heat exchangers. Heat transfer plays a crucial role in determining the performance of such devices and has therefore been a subject of numerous investigations over the past few decades. These studies addressed fluid-packed particle heat transfer, transient response of PBHS and various effective parameters under the steady-state including effective axial and radial thermal conductivities, wall to fluid heat transfer coefficient and overall heat transfer coefficient. These effective parameters are obtained by solving the inverse problems using various macroscopic models. The simplest macroscopic model is one-dimensional and contains an overall heat transfer co efficient (U) based on the difference between the radial average temperature of the particle bed and the corresponding wall temperature (Wen and Ding, 2006).

Many systems in science and engineering are distributed in space and time, and as a consequence, can be described by sets of, generally nonlinear, partial differential equations. These mathematical models usually involve several unknown parameters whose numerical values must be inferred from experimental data. Of course, the information content of the measurement is a primary determinant of the accuracy of the parameter estimates and particular attention must be paid to the careful design of experiments. (Vande Wouwer *et al.*, 2000).

When designing and optimizing a process or a system, mathematical models are useful for a better understanding of the dynamic (unsteady state) and static (steady state) behaviors. Mathematical models have the potential to prove general results; these results depend critically on the form of equations used. Small changes in the structure of equations may require enormous changes in the mathematical methods. Using computers to handle the model equations may never lead to elegant results, but it is much more robust against alterations.

## I.2 AIM

The main goal of this study is to develop a mathematical model for determining temperature distribution and heat loss in a PBHS tank where the heat transfer mechanisms are conduction, advection, forced convection and free convection. Using the developed model, the effect of axial dispersion, natural and forced convection and their contribution to the efficiency of the heat storage will be investigated.

Developing a reliable mathematical model for the PBHS system used in this study will be a great asset for researchers who intend to study in similar cases, since there is little explanation in the literature relating how axial dispersion and free convection concepts are affecting PBHS systems. Having a reliable mathematical model and optimized PBHS system will greatly enhance the capabilities of the researchers to apply the same model in any PBHS system.

# CHAPTER II

## GENERAL BACKGROUND

In this chapter, heat storage and heat transfer mechanisms during storing sensible heat in a packed bed will be explained briefly. Additionally, previous studies in the literature relating PBHS systems will be discussed.

### II.1 HEAT STORAGE:

Efficient energy storage facilitates the integration of renewable energy sources into energy systems. By using heat storage system, the production of electricity and heat can be un-coupled for a period of time depending on the size of the heat storage. Because of temporal variability in the availability of solar and industrial process heat, thermal storage systems are key components for the effective utilization of this heat in solar thermal power stations, heat recovery processes, solar local heat projects, air-conditioning systems in buildings, and service water systems.

#### II.1.1 Thermal Energy Storage

The amount of the stored thermal energy depends on the thermal storage system's dimensions, energy storage type and thermal energy storage materials. Thermal energy can be stored as sensible and latent heat. The capacity of the storage system is determined by considering the amount of required and obtained thermal energy. The temperature variation and thermal energy storage capability of the storage material are main factors in *sensible heat storage*. Sensible heat storage is in common use because of its easy and economical application.

In sensible heat storage, the water is widely used as storage material because, it can be supplied easily everywhere and it has no negative property except corrosion. The water has also high volumetric specific heat so that, higher amount of thermal energy can be stored per unit volume. The water temperature inside the storage tank depends on amount of thermal energy, which enters the tank and exit from the tank.

The variation of the water temperature inside the tank is related with thermal capacity of water inside the tank, amount of energy enter to and exit from the tank and heat loss from the surfaces. The vertical temperature variation inside the tank leads to a thermal stratification. The thermal stratification is very important in solar energy storage tank. Higher thermal stratification causes better the performance of the hot water storage system (Altıntop *et al.*, 2006).

### II.1.2 Packed Bed Heat Storage for Storing Sensible Heat

In energy systems where a temporal difference exists between the supply of energy and its utilization, some form of energy storage is necessary to insure the continuity of a thermal process. Both waste heat recovery and solar thermal energy systems are primary applications for thermal energy storage. For air systems and in the case of this study, liquid system such as water heating, a packed bed provides effective thermal energy storage. In general, a packed bed receives energy during its charging cycle from a heated fluid and releases the same energy by discharging cycle when it is needed (Beasley and Clark, 1984).

A packed bed system for storing sensible heat consists of a storage medium, a container and input/output devices. Containers must both retain storage material and prevent loss of thermal energy. The phenomenon of thermal stratification must intervene at this point due to the desire to obtain thermal gradient across the storage medium. The amount of energy stored by a sensible heat storage system is proportional to the difference between the storage input and output temperatures, the mass of the storage medium and the heat capacity of the storage material (Dincer *et al.*, 1997).

Figure II.1 is a schematic presentation of the packed bed heat storage system used in all the steps of this present study.

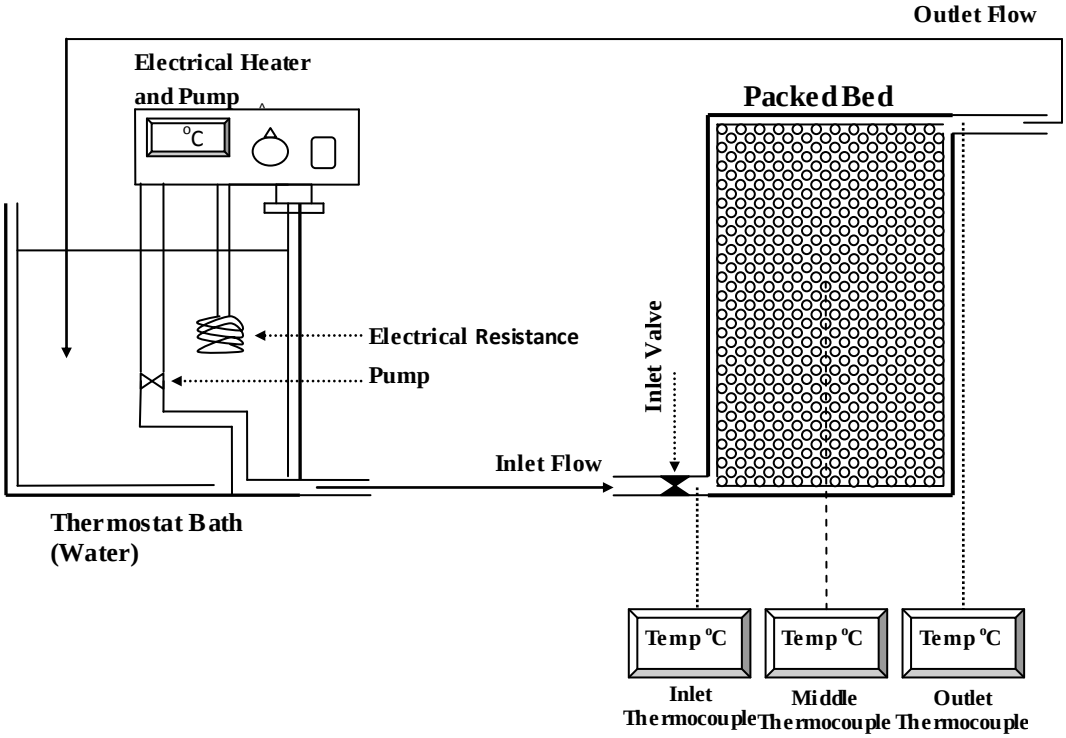


**Figure II.1 Simple schematic design of the packed bed heat storage system**

### II.1.3 Heat Transfer Mechanisms during Sensible Heat Storage in a Packed Bed

The mechanisms of heat transfer in a packed bed for storing sensible heat consist of heat conduction, advection, convection and free convection (radiation is neglected). When the aim is developing a mathematical model for such cases, the developed model should be included with the mathematical expressions of these heat transfer mechanisms. Of course, regarding a complete representation of any packed bed heat transfer phenomena by mathematical modeling, the expressions must be in three dimensional (3D). The experimental atmosphere and conditions, forced researchers to make necessary neglecting and limitations on the mathematical model.

#### Heat Transfer by Conduction

When a temperature gradient exists in a body, physics have shown that there is an energy transfer from the high-temperature region to the low-temperature region. It is said that the energy is transferred by conduction and that the heat transfer rate per unit area is proportional to the normal temperature gradient:

$$\frac{q}{A} \sim \frac{\partial T}{\partial x} \qquad \text{(II. 1)}$$

When the proportionality constant is inserted it becomes,

$$q = -k_m A \frac{\partial T}{\partial x} \qquad \text{(II. 2)}$$

Where;

$q$ : The heat transfer rate (J/s)

$\partial T/\partial x$ : The temperature gradient in the direction of the heat flow

$k_m$ : The thermal conductivity of the material (J/smK)

A : Heat transfer area ($m^2$)

The minus sign is inserted so that the second principle of thermodynamics will be satisfied. Equation (II.3) is called Fourier's law of heat conduction after the French mathematical physicist Joseph Fourier (Holman, 1983).

**Heat Transfer by Advection**

The movement of a quality, such as heat, or humidity, due to the flow of the fluid possessing that property is simply defines the concept of advection. When a fluid flows through any system, heat transfer occurs due to this movement. The rate of this heat transfer depends on the velocity, density, specific heat capacity and the changing temperature of the moving fluid. Especially, in the case of sensible heat storage in a packed bed, heat transfer by advection plays a considerable role for an accurate mathematical model.

$$\dot{q} = \rho_f C_f v_z \frac{\partial T}{\partial z} \qquad \text{(II. 3)}$$

Where;

$C_f$ : Heat capacity of the fluid (J/kgºC)

$\rho_f$ : Fluid density ($kg/m^3$)

$V_z$ : Fluid velocity (m/s)

**Heat Transfer by Convection**

It is well known that a hot plate of metal will cool faster when placed in front of a fan than when exposed to still air. It is said that the heat is convected away and the process is called convection heat transfer. The term *convection* provides an intuitive notion concerning the heat transfer process; however, this intuitive notion

must be expanded to arrive at anything like an adequate analytical treatment of the problem.

Consider the heated plate shown in Figure (II.2). The temperature of the plate is $T_w$ and temperature of the fluid is $T_\infty$ the velocity of the flow will appear as shown, being reduced to zero at the plate as a result of viscous action. An analytical calculation of ***h*** may be made for simple systems. For complex situations it must be determined experimentally (Holman, 1983).

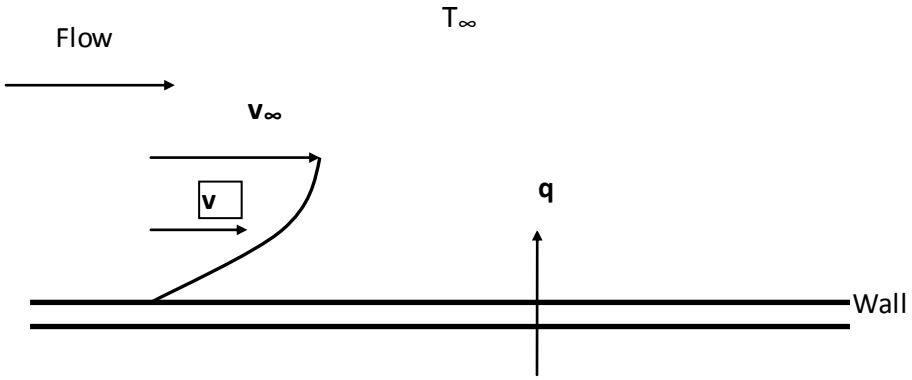


**Figure II.2 Convective Heat Transfer on a Wall Surface**

To express the overall effect of convection, Newton's law of cooling is used:

$$q = hA(T_w - T_\infty) \qquad \text{(II.4)}$$

Where;

$h$ : Convective heat transfer coefficient (J/m$^2$ s K)

$T_w$ : Temperature of the wall (K)

$T_\infty$ : Outside temperature (K)

**Heat Transfer by Natural Convection**

Free or natural convection is observed as a result of the motion of the fluid due to density changes arising from the heating process. A hot radiator used for heating a room is one example of a practical device which transfers heat by free convection. The movement of the fluid in free convection, whether it is a gas or a liquid, results from the buoyancy forces imposed on the fluid when its density in the proximity of the heat transfer surface is decreased as a result of the heating process. The buoyancy forces would not be present if the fluid were not acted upon by some

external force field such as gravity, although gravity is not the only type of force field which can produce the free convection currents; a fluid enclosed in a rotating machine is acted upon by a centrifugal force field, and thus could experience free convection currents if one or more of the surfaces in contact with the fluid were heated. The buoyancy forces which give rise to the free convection currents are called body forces (Holman, 1983).

Natural convection will be more likely and/or more rapid with a greater variation in density between the two fluids, a larger acceleration due to gravity that drives the convection, and/or a larger distance through the medium. Therefore, natural convection is determined by Rayleigh number which is modified in the present case for thermal expansion and thermal diffusivity. Further information can be found in Chapter V and Appendix D.

## II.2 LITERATURE SURVEY

At this level of the present study, most of the related studies in the literature were investigated and they are presented here. These studies are grouped for the reader to follow easily.

### II.2.1 Foundations of the Present Study

One of the pioneering works on the modeling of packed bed heat storage unit was done by Beasley and Clark (1984). They have presented a two dimensional model for the fluid phase and time dependent model was considered for the solid phase. In addition to the thermal dispersion effects in the axial and radial directions, the model also considered the effect of the heat transfer through the packed bed wall. They have tested their model results with the results obtained from experiments done using a rock-bed and air as working fluid. In the model equations the void fraction, fluid velocity and transport coefficients were considered to be changing spatially. They calculated the Nusselt number (*Nu*) using the results of separate experiments and they have concluded that the experimental results fitted better the model results when 50% higher values of the Nu were used. The experiments were performed at temperatures from 25 to 60°C and for a range of superficial Reynolds number (*Re*) from 90 to 660. The superficial Reynolds number is calculated using the superficial fluid velocity. However no pertinent information concerning the radial and axial thermal dispersion effects were given.

A study on the utilization of granular phase change composites (GPCC) in latent heat thermal energy storage (LHTES) systems was done using a mathematical model (Rady, 2009). The model was time dependent and one-dimensional and it consists of the terms representing heat transfer by axial dispersion, advection and convection. After the modeling, the effects of phase change characteristics, bed porosity and fluid-to- particle heat transfer coefficient and axial dispersion were investigated. According to experimental results, the model was not in agreement with the expectations considering the effect of phase change characteristics. However, the effect of bed porosity was found significant. Relating the effects of fluid-to-particle heat transfer coefficient, some uncertainties were observed due to used correlation and assumptions. It was also obtained that axial dispersion has no significant effect because the longitudinal thermal dispersion did not contribute to the overall thermal response of the packed bed. It was concluded that accurate prediction of porosity is essential for developing a reliable model (Rady, 2009).

Thermal dispersion in a bed of glass beads was studied with the purpose of investigation of the effects of heat diffusion in fluid and solid phases and thermal convection of the fluid (Testu *et al.*, 2007). The originality of this study was adding the hydrodynamic effect of the flow through the column as one of the investigation parameters. At the modeling stage, *one –temperature* model was used. For the experimental part of the study, a column where the fluid was passing through was contained with glass beads of 2 mm diameter and an iron electrical resistance wire (for heating) was used.

Determination of thermal-dispersion coefficient for *one-temperature* model can be made numerically and also it was suggested that the information of fluid-solid interface structure, thermo-physical properties of two phases and fluid velocity structure were needed. For the experimental part of the study, estimating the thermal dispersion coefficient came together by comparing the temperature residual graphics and Peclet number ($Pe$=30) with experimental data. And the accordance between *one-temperature* model and experimental work was observed. Finally, it was proved that thermal-dispersion coefficient was highly depended on thermo-physical properties of liquid and solid material structure of the porous medium and flowing velocity of the fluid (Testu *et al.*, 2007).

In a similar study, the heat transfer behavior of a gas flow through a packed bed by means of effective parameters such as effective axial and radial thermal

conductivities, wall to fluid heat transfer coefficient and overall heat transfer coefficient was investigated. One–phase homogeneous model was used due to small temperature difference between the bulk fluid phase and the solid phase. The packed bed was investigated with the aspects of pressure drop of gas through the bed, temperature profiles inside the bed and derivation of effective heat transfer parameters. Based on the used correlation for estimating the axial effective thermal conductivity (thermal dispersion coefficient), very small errors were found which was considered to be acceptable. It was proved that one-phase homogenous two dimensional axial dispersion plug flow model (2DADPF) showed very good agreement with axial temperature distribution, although the model has less satisfactory particularly in the region close to inlet (Wen and Ding, 2006).

One of most popular study was based on the investigation of the influence of fluid dispersion coefficients on particle-to-fluid heat transfer coefficients. The importance of this work is to be the pioneering study for using the axial dispersion coefficient while combining the both laminar and turbulent flow behaviors. The used heat transfer measurements in this study included high Reynolds numbers up to 8500. For such high flow rates one of the reliable axial fluid dispersion definitions was obtained. After the evaluation of mentioned statements and plotting the correlated data as Nu vs. Re, the below relation was proposed (Wakao, 1979);

$$Nu = 2 + 1.1 Pr^{\frac{1}{3}} Re^{0.6} \qquad \text{(II. 5)}$$

It can be concluded from the study that when the purpose is to investigate heat transfer behavior of packed beds, the given correlation must be taken into consideration (Wakao, 1979).

Thermal hydraulic characteristics of thin annular pebble beds in terms of radial and axial gas flow was a subject of another study. It was aimed on two cases, one of them was the case of axial gas flow and the other was the radial gas flow thorough the pebble bed. The purpose of the investigation of axial gas flow was determining hydraulic drag of thin annular pebble beds and the heat transfer coefficient from spheres of various diameters. And the investigation of the radial flow was about the distribution of the flow along pebble bed. An average heat transfer coefficient was determined by using local modeling method. Due to high working range of *Re*,

natural convection considered negligible. As a measure of pressure drop, *hydraulic drag* was calculated (Rimkevicius *et al.*, 2007).

From the aspect of axial flow it was concluded that when designing heat exchanger with annular bed the value of *Nu* must be known. Thus, they investigated Nu values for different *Re* values. Considering radial flow they it was observed that minimizing the pressure drop is possible. In this case uniform flow distribution along the pebble bed was essential. Increasing hydraulic drag has no effect on the regulation of the flow distribution. Although, by keeping in mind that without causing an increase in common hydraulic drag, it was possible to achieve flow distribution equalization by smooth changes of hydraulic drag in the outlet header (Rimkevicius *et al.*, 2007).

### II.2.2 Axial Dispersion Coefficient Functions

In the literature, there are various studies which are emphasizing the axial dispersion coefficients to be used in modeling of PBHS systems. In the present study, some elegant approaches will be demonstrated for this purpose.

Table II.1 shows some of those approaches that compatible for the present study.

**Table II.1 Axial Dispersion Correlations**

| The References | Axial Dispersion Correlation Functions |
|---|---|
| Wakao, (1981) | $k_d = \left[\frac{k_f}{\varepsilon C_f \rho_f} + 0.5 D_p V_z\right] \varepsilon C_f \rho_f$ |
| Wen and Ding, (2006) | $\frac{k_d}{k_f} = \frac{k_e}{k_f} + 0.5 Re_p Pr$ |
| Aris-Taylor, taken from Fogler, (2005) | $k_d = k_f \left\{1 + \frac{1}{48}\left[\left(\frac{V_z D_p/2}{k_f/\rho C_p}\right)^2\right]\right\}$ |

where

$k_d$ : Axial dispersion coefficient (J/m s K)

$k_e$ : The thermal conductivity of a quiescent bed (J/m s K)

$k_f$ : Fluid thermal conductivity (J/m s K)

$D_p$ : Particle diameter (m)

ε : Void fraction of packed bed

$Re_p$ : Reynolds number (particle diameter based) (m/s)

In this thesis, all of these three approaches are used. Also, the comparisons of the results are made in Chapter V. Although it can be said briefly that the approach of Wakao *et al.* (1981) was found to be the best fitting equation for the model that is used in this study.

### II.2.3 Nusselt Number Correlations for determining the value of *h*

It was mentioned before that the determination of the convective heat transfer coefficient, ***h*** can be made analytically, but in the case of packed beds, it must be obtained experimentally due to number of interactions along the bed. Many scientific works can be found in literature for determination of *h* experimentally by using different Nusselt number correlations. Table II.2 includes the most used Nusselt number correlations.

**Table II.2 Nusselt number correlations**

| The References | Correlation Function |
|---|---|
| Wakao, (1979) | $Nu = 2 + 1.1Pr^{1/3}Re^{0.6}$ |
| Gunn, (1978) | $Nu = 4\left(1 + 0.7Pr^{\frac{1}{3}}Re^{0.2}\right) + 0.6Pr^{1/3}Re^{0.7}$ |
| Hanrattry, (1954) | $Nu = \frac{1.1}{\varepsilon^{1/2}}[6(1-\varepsilon)]^{1/2}Re^{1/2}Pr^{1/2}$ |

Where,

*Nu* : Nusselt number ($Nu=hD_p/k$)

*Re* : Reynolds number ($\rho D_p V_z/\varepsilon\mu$)

*Pr* : Prandtl number ($C_p\mu/k$)

$\mu$ : Viscosity (kg/m s)

To be able to see the behavior of these correlations as a function of Re the Figure II.3 is given.

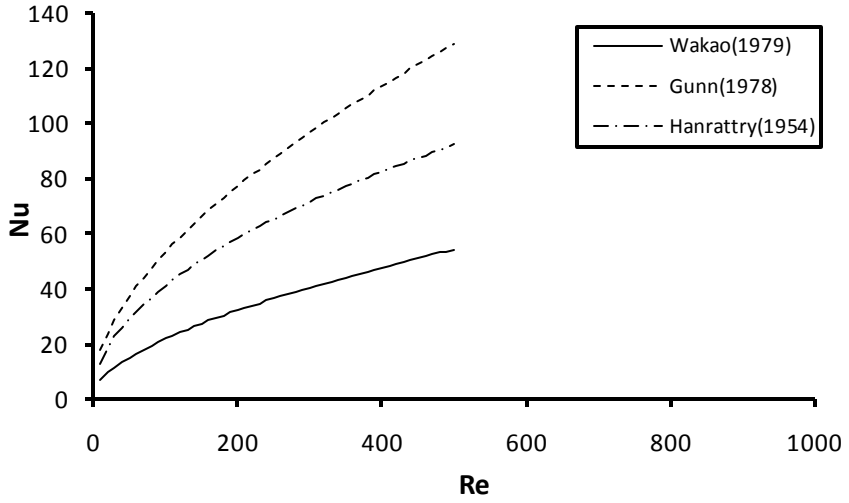


**Figure II.3 Nusselt number correlations**

The range of the Reynolds values in Figure II.3 is in satisfactory, since the Reynolds values in the present study ranges 10 to 60. It can be seen that all three correlation functions behaves differently, due to different assumptions, different experimental setup and etc.

What is beneficial for the present study is that these correlations are helpful when investigating the effect of the variable *h* in the mathematical model, since, Nusselt number is a function of convective heat transfer coefficient.

### II.2.4 Free and Mixed Convection

For the purpose of examining free convection effects in heat transfer, the influence of free convection at high Rayleigh numbers was investigated on the basis of a computational model (Huynh, 2006). The study was performed using of heated circled cylinder positioned above a horizontal plane. Throughout this investigation turbulence effect was not neglected, thus a Reynolds-Average Navier-Stokes formulation was used for such high Rayleigh numbers. The investigator observed that when the gap ratio (*h/D*) values were reduced *Nu* increased to a maximum, and this maximum occurred closer to the cylinder at higher *Ra*. As the value of *h/D* was reduced further, values of Nu decreased to a minimum then increased again as the cylinder's surface was approached. After experimental work, it was concluded that thermal condition of the underlying plane has insignificant effect on the heat transfer

from cylinder's surface at low values of gap ratio. The significant effect of the underlying plane was observed at high values of *h/D* (Huynh, 2006).

Based on the approach of that laminar flow through a vertical pipe will always be unstable, when inlet boundary conditions are changing with time, mixed convection in vertical pipe was investigated.

One of the other significant study examined mixed convection heat transfer in vertical packed channel (Pu *et al.*, 1999). Using asymmetric heating method a vertical channel of packed bed is heated in the range of $2<Pe<2200$ and $700<Ra<1500$. After interpreting the results with the range of given Pe and Ra numbers, the following three convection regimes were obtained:

Natural Convection Regime: $105<Ra/Pe$

Mixed Convection Regime: $1<Ra/Pe<105$

Forced Convection Regime: $Ra/Pe<1$

These regimes were observed along the length of the packed channel. This was an inspiring study for the present thesis, since both free and forced convection is observed at the experimental stage.

### II.2.5 Thermocouple Location

A sensor location criterion was developed for placing the thermocouples in a catalytic fixed bed reactor. Optimal sensor locations were investigated on the basis of state estimation and parameter estimation. One of the made approaches for developing optimality criterion, collected sensor data was hold at maximum level while sensor output correlations was hold minimum level. The obtained optimality criterion was used to determine the optimal locations of the thermocouples. It was concluded that it is very useful to use optimality criterion when locating thermocouples or any other sensors (Wouwer, 2000).

### II.2.6 Energy and Exergy Analysis of Packed Beds

For determining thermal efficiency and performance of a thermal energy storage system (TESS), energy and exergy analysis were made. The exergy efficiency is a measure of how nearly a system approaches ideal performance. It was suggested that when proving the performance of a TESS, focusing the exergy analysis is more reliable than focusing on energy analysis. Because exergy analysis

answers the questions of how practical and how acceptable is your TESS (Dincer *et al.*, 1997).

In another similar study, it was suggested that the experimental results can be used for thermodynamically evaluation of any packed bed system. The aim was to make a thermal behavior comparison of zirconium oxide ($ZrO_2$) as a sensible-heat material (SHM) and salt/ceramic composite ($Na_2SO_4/SiO_2$) as a phase change material (PCM) at high temperatures. In conclusion, due to high thermal capacity of zirconium oxide offers thermodynamically superior performance over the composite material. And including other aspects of this study zirconium oxide appears to be more promising than the used PCM (Jalalzadeh-Azar *et al.*, 1997).

Focusing on minimizing the irreversibilities in the storage system by using the concept of exergy was a subject of a similar study. In order to minimize the irreversibilities, it was needed to obtain optimum operational conditions for various operation parameters. Storage system used in this work consists of an isolated liquid bath, electrical heater inside the bath and a heat exchanger through the bath. The first law analysis and the second law analysis of the system were made and it was concluded that only modifying the storage process made it possible to improve the second law efficiency, thus to minimize the irreversibilities. It was also observed that the highest irreversibility occurs due to heat transfer between the discharged gas and atmosphere and due to temperature difference between the liquid bath and gas (Biyikoglu, 2002).

### II.2.7 Inlet Fluid Velocity and Thermal Stratification

High thermal stratification and long-term usage of mantled hot water storage tank is investigated for proving the agreement between the used model and the experimental work for specific fluid velocities. The behavior of thermal stratification was examined at un-steady state for 12 different inlet velocities. The investigation showed that the temperature difference between inlet and outlet of the tank at low inlet velocities was higher with respect to the temperature difference at high inlet velocities. It was suggested that the cause of this situation was the rise of the hot water region at the top of tank due to increase of the inlet velocity. After all the experimental work, it was proved that increasing the water velocity causes increasing the heat transfer coefficient (Altuntop *et al.*, 2006).

# CHAPTER III

## MATHEMATICAL MODELING

In this chapter, mathematical modeling of the study will be presented. The mathematical model will be analyzed in the aspects of the made assumptions, the physical properties of fluid and solid, effect of natural and forced convection, the model parameters and the bed properties.

### MODEL DEVELOPMENT

The mathematical model that is used in the present study is based on the model which is given in Appendix C. The foundation of the model relates itself to the phenomena of one-dimensional heat transfer equation which is explained elaborately in Appendix A. The derivation of the mathematical model is also given in Appendix C. The model given in Eq. (C.5) is widely used in literature for different kinds of packed bed systems and it is found very convenient for the PBHS system that is used in this study. It includes all the necessary concepts of heat transfer mechanisms that take place in the present PBHS system.

#### Mathematical Model

The adjusted model used in this study includes particular modifications of the model which is given in Eq. (C.5) due to the specific assumptions for simplifying the present PBHS system. The purpose of simplifying assumptions is to reduce the number of parameters and the number of variables appearing in the model equations.

#### Simplifying Assumptions

- Heat transfer mechanisms are only present in axial and radial directions.
- Temperature distribution in radial direction along the packed bed is neglected.
- Heat losses during the transportation of the fluid to the tank from the thermostat are neglected.

- Velocity of the flowing fluid is constant across the packed bed system and there are no wall effects.
- Packed bed particles (glass beads) are randomly packed. And, constant void fraction ε, is used for random packing.
- Physical properties of the fluid such as density, heat capacity, viscosity and heat transfer coefficients change with temperature.
- Overall heat transfer coefficient *U* changes with temperature.
- Axial dispersion coefficient $k_d$ includes both effects of axial dispersion and contribution of the natural convection to the axial dispersion.
- Temperature distribution along the diameter of any individual particle is neglected.

**The Model**

The second term of Eq. (C.5) which includes the radial thermal distribution along the bed was neglected in the present model due to difficulties of measuring the radial temperature distribution and less participation to the free convection mechanism. And additionally, a new term was added to the Eq. (C.5) which represents the heat losses from the system to the surrounding air by using overall heat transfer coefficient, *U*. After these modifications the following model equations were obtained for thermal distribution of the fluid and thermal distribution of the solids respectively:

$$\varepsilon\frac{\partial\left(\rho_f C_f T\right)}{\partial t} = \frac{\partial}{\partial z}\left(k_d \frac{\partial T}{\partial z}\right) - \varepsilon\frac{\partial\left(\rho_f C_f V_z T\right)}{\partial z} - ha(T - T_s) - Ua_t(T - T_{air}) \quad \text{(III. 1)}$$

$$(1-\varepsilon)\rho_s C_s \frac{\partial T_s}{\partial t} = ha(T - T_s) \quad \text{(III. 2)}$$

Where,

$z$ : Axial direction

$r$ : Radial direction

$t$ : Time (s)

$C_s$ : Heat capacity of the solid (J/kg ºC)

$\rho_s$ : Solid density (kg/m$^3$)

$T$ : Temperature of the fluid (ºC)

$T_s$ : Temperature of the solids (ºC)

$U$ : Overall heat transfer coefficient (J/m$^2$ ºC)

$A$ : Specific surface area of glass beads, 6(1-ε)/$D_p$ (1/m)

$a_t$ : Specific heat transfer surface ($S_t/V_t$) (m$^2$/m$^3$)

Eq. (III.2) represents the changes of temperature of the solid particles with time. In the present model, Eq. (III.1) and Eq. (III.2) were used simultaneously.

For a better understanding of the model, it is useful to explain the model in the basis of energy balance. The present mathematical model is based on the following differential energy balances which represent Eq. (III.1) and Eq. (III.2) respectively:

$$\left\{\begin{matrix}Rate\ of\ change\\ of\\ heat\ content\ of\\ the\ fluid\end{matrix}\right\} = \left\{\begin{matrix}Heat\ transfer\\ rate\\ due\ to\ thermal\\ dispersion\end{matrix}\right\} - \left\{\begin{matrix}Heat\ transfer\\ rate\\ due\ to\\ advection\end{matrix}\right\} - \left\{\begin{matrix}Convective\ heat\ transfer\\ rate\ between\\ the\ packing\ material\\ and\ flowing\ fluid\end{matrix}\right\} - \left\{\begin{matrix}Convective\ heat\ transfer\\ between\ the\ flowing\ fluid\\ and\ the\ surrounding\ air\\ through\ the\ packed\ bed\ wall\end{matrix}\right\} \quad \text{(III. 3)}$$

$$\left\{\begin{matrix}Rate\ of\ change\ of\\ heat\ content\\ of\ the\\ packing\ material\end{matrix}\right\} = \left\{\begin{matrix}Convective\ heat\ transfer\\ rate\ between\\ the\ fluid\\ and\ the\ packing\ material\end{matrix}\right\} \quad \text{(III. 4)}$$

The developed model represented by Eq. III.1 and Eq. III.2 was solved numerically using finite difference method which is explained in Appendix B.

# CHAPTER IV

## EXPERIMENTAL WORK

In this chapter, the experimental set up and procedure of performing the experiments will be presented. In all experiments fluid inlet temperature and fluid flow rate thus the fluid velocity are the manipulated variables to check the effect of the model parameters such as the thermal dispersion coefficient $\mathbf{k_d}$ and the convective heat transfer coefficient **h** on the experimental results. The experiments are performed as cooling and heating experiments depending on the inlet fluid temperature and the initial temperature of the packed bed.

### IV.1 EXPERIMENTAL SET UP AND SYSTEM GEOMETRIES

Heat storage system is composed of the thermostat and packed bed heat storage tank. Furthermore the packed bed heat storage tank was composed of the glass beads as the packing material and the thermocouples.

The tank was made up of stainless steel and has cylindrical geometries. As it is shown in Figure IV.1 there is one inlet pipe at the down side of the tank and one outlet pipe at the upper side of the tank. The inlet flow rate was controlled by a valve and a centrifugal pump was used to transport the working fluid.

Thermocouple system consists of three temperature indicator (Pt1000 heat couple) screen which reflects the temperatures measured by thermocouples. The three thermocouples were placed in the tank; one of them at the inlet, one of them at the outlet and the other at the centre of the tank along with the glass beads. The location of the thermocouple placed at the centre of the tank is adjustable. During most of the experiments, this movable thermocouple was placed right at the top of the packed bed to measure the experimental outlet temperature. The location of the other two thermocouples was fixed during all the experiments.

For the heat storage part of the system, glass beads were used for storing heat. The tank was filled from the bottom to the top with glass beads by poured random packing style.

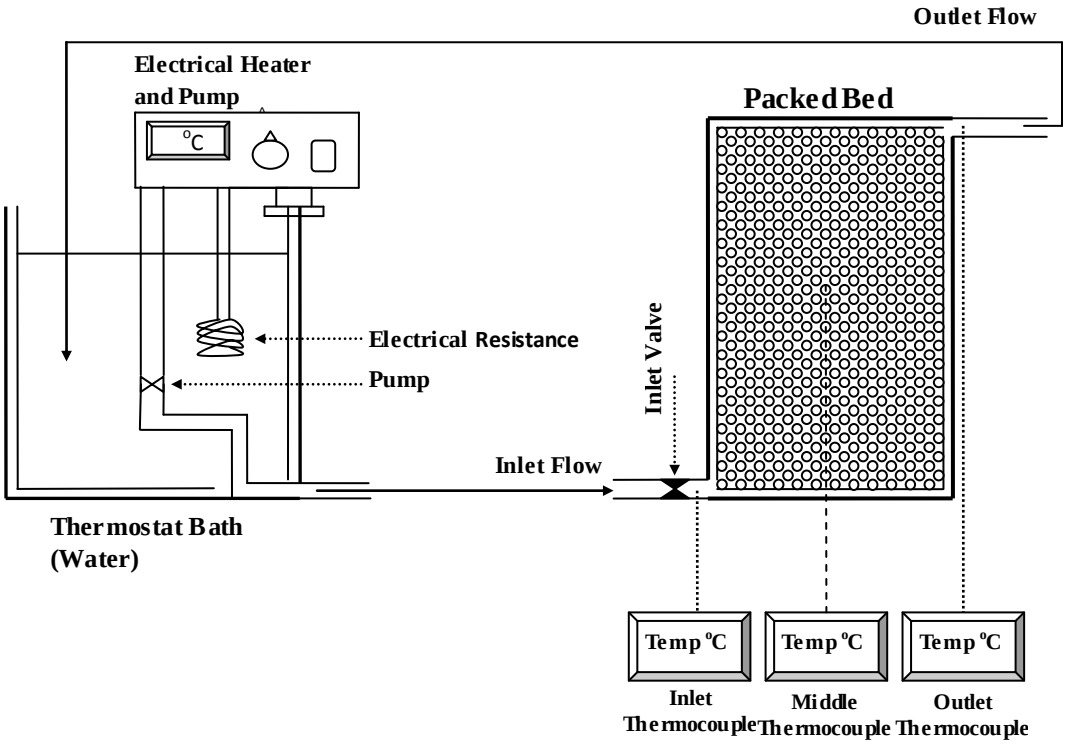


**Figure IV.1 Simple schematic design of the experimental setup used in all experiments**

Table IV.1 includes the dimensions and properties of all the parts of the used system in this work. The properties of the flowing fluid (water) will be given in below pages separately.

**Table IV.1 Dimensions and properties of the experimental system**

| | $\rho$ (kg/m$^3$) | $C$ (kJ/kg°C) | $k$ (J/ms°C) | $h$ (J/m$^2$s°C) | Height (m) | Diameter (m) | Volume (m$^3$) |
|---|---|---|---|---|---|---|---|
| **Tank** | 7850 | 0.502 | 16 | --- | 0.235 | 0.223 | 0.0092 |
| **Glass Beads** | 2400 | 0.840 | 0.96 | --- | --- | 0.026 | --- |
| **Air** | 1.205 | 1.005 | 0.0257 | 1.0 | --- | --- | --- |

## IV.2 EXPERIMENTAL PLAN

The purpose of the experiments is to investigate the temperature distributions across the packed bed while charging (heating) and discharging (cooling).

The heated water from the thermostat is charged to the packed bed at constant flow rate and temperature during charging process. The flow rate is adjusted and fixed by the valve at the inlet. For the purpose of maintaining the temperature of the thermostat constant, the other edge of the outlet pipe is returned inside the pool of the

thermostat. And the indicated temperatures are recorded every fifteen seconds until the outlet temperature reaches to the charging temperature (fluid inlet temperature). As soon as the charging process is done, the discharging process is begun since a heated bed is already at hand. The inlet pipe is plugged out from the thermostat and connected to the city water during discharging. And the outlet water is released to the sink. While discharging process continues the thermostat is adjusted to a new or the same charging temperature, to be able to use after discharging. And the indicated temperatures are recorded in the same way as during the charging.

The mentioned procedure was used during all experiments and Table IV.2 represents the performed experiments at different temperature ranges and flow rates. Here, the observed effect of flow rate and temperature range on the durations of the experiments is shown.

**Table IV.2 List of experiments**

| Exp. | Process | Temperature Range (°C) | Flow Rate (L/s) | Duration (s) |
|---|---|---|---|---|
| **1.** | Heating | 15-30 | 0.0078 | 1230 |
| **2.** | Cooling | 45-15 | 0.0078 | 1785 |
| **3.** | Heating | 15-45 | 0.0094 | 1485 |
| **4.** | Cooling | 40-15 | 0.0148 | 1155 |
| **5.** | Heating | 15-55 | 0.0166 | 1020 |
| **6.** | Cooling | 55-15 | 0.0166 | 900 |
| **7.** | Heating | 20-40 | 0.0202 | 870 |
| **8.** | Cooling | 55-15 | 0.0148 | 1155 |
| **9.** | Heating | 15-29 | 0.0202 | 765 |
| **10.** | Cooling | 30-15 | 0.0078 | 1425 |

**Input Variables**

The input variables for the present study are changing ranges of inlet temperature and flow rate ($V_z$). Almost every experimental step of the present work was performed for different temperature ranges and flow rates. The effects of these input variables are related to thermal dispersion across the tank and will be investigated in Chapter V.

# CHAPTER V

## RESULTS AND DISCUSSIONS

In this chapter, the obtained results using the present model will be compared to the experimental results. All of the significant and relevant aspects of the experimental results are considered and will be discussed with conjunction to the behavior of the present model.

Also, thermal behavior of the mathematical model, effect of the fluid velocity, thermal behavior of the bed during discharging and charging, and the effects of input such as the inlet temperature and water flow rate variables on the temperature profiles will be examined. Additionally, when the word *"temperature"* is used in the following pages, it is always referred as the fluid temperature, unless there is no additional indication.

### V.1 DYNAMIC BEHAVIOR AND PARAMETERS OF THE MATHEMATICAL MODEL

Using the model, different parameters taking place in the model equations can be analyzed. In addition, their effect on the model output such as the water and packing material temperatures can be presented. The input variables of the model are the temperature and flow rate of the inlet water (heating and cooling medium fluid). The velocity of the water along the bed varies as the temperature and thus the density of the water changes. Therefore the model and experimental results are presented for different water inlet temperatures and Reynolds number at the inlet conditions. In addition there are model parameters taking place in the model equations. These parameters determine the shapes of the temperature profiles along the packed bed with time and thus the duration of the heating and cooling cycles. The effect of the model parameters will be explained in the following section in detail.

### V.1.1 Effects of the Model Parameters

The significant parameters taking place in the model equations are the fluid velocity $V_z$ (which is a function of the inlet water flow rate and temperature due to viscosity changes), convective heat transfer coefficient $h$, and axial dispersion coefficient $k_d$ due to their contribution to the behavior of the temperature variation along the bed.

Density of the fluid $\rho_f$ and the solid $\rho_s$, heat capacity of the fluid $C_f$ and solid $C_s$, convective heat transfer coefficient $h$ and overall heat transfer coefficient $U$ were all calculated along the bed length with time. Since, the maximum temperature difference is 40 ºC for the present work, the values of these parameters were considered as temperature dependent. Thus, determination of their values and temperature dependent functions are shown and explained in Appendix D.

### V.1.2 Axial Dispersion Coefficient "$k_d$"

Using the axial dispersion correlation functions given in Table II.1 the present model was run on the software Matlab®. The correlation of Wen and Ding (2004) is behaving a little different as the correlation is proposed for air as the working fluid. After searching the literature, the axial dispersion coefficient correlation of Wakao *et al.* (1981) is compared with other correlations and found acceptable. This correlation was used at all calculation steps of the model. Figure V.1 shows the difference between these most known correlations in the literature. The accuracy of choosing the correlation of Wakao *et al.* (1981) will be seen more obviously in following pages while discussing heating and cooling processes.

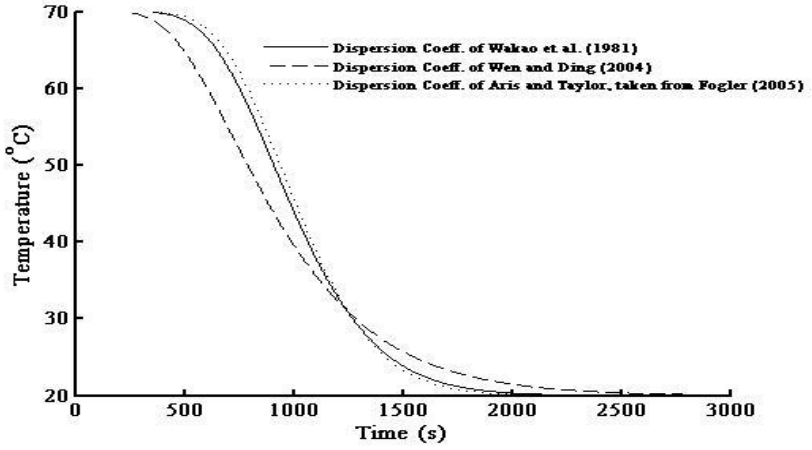


**Figure V.1 Axial fluid outlet temperature profiles obtained from a cooling simulation for different thermal dispersion correlations (Re=14, Flow rate=0.0078 L/s,)**

### V.1.3 Convective Heat Transfer Coefficient "*h*"

Convective heat transfer coefficient ***h*** is related to Nusselt number varying along the packed bed. The relation is given in Appendix D, using the Nusselt number correlations in Table II.2, the present model was run on the software Matlab®. The results were plotted in Figure V.2 to show that there is no significant variation between the used correlations. Nusselt number correlation of Hanrattry (1954) is chosen to be used in the present study, since it includes the parameter of void fraction. Also, Appendix D includes derivation of specific surface area of glass beads "a" and specific heat transfer surface "$a_t$".

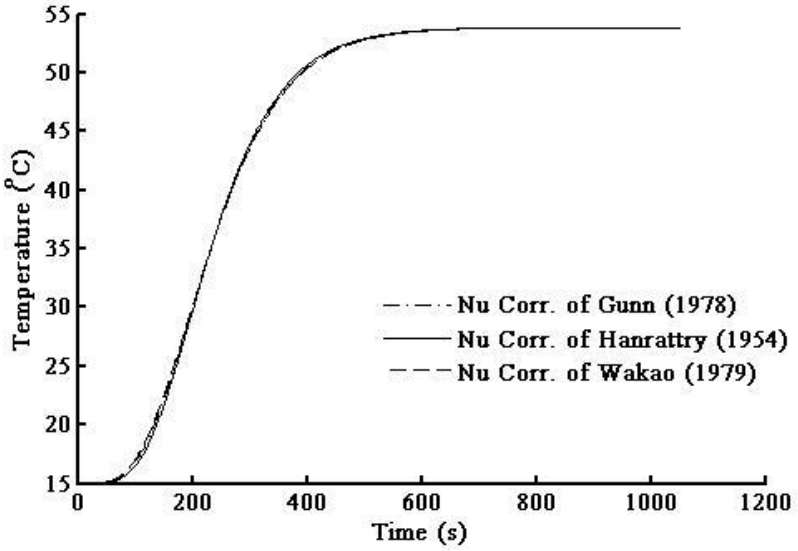


**Figure V.2 Comparison of Nusselt number correlations for a heating simulation (Re=43, Flow rate=0.166 L/s, $T_{in}$=55°C)**

### V.1.4 Packed Bed Properties

Determination and replacing the packed bed properties into the mathematical model is crucial for obtaining accurate results. Since, the dimensions of the packed bed are known and can be used accurately, using the true value of void fraction "$\varepsilon$" is essential.

#### Void Fraction of the Packed Bed

In the literature, void fraction is modeled as an exponential decay function which is referred as the average bed porosity. The model is given by the following equation (Klerk, 2003).

$$\varepsilon = \varepsilon_b + 0.35exp\left(-0.39\frac{D}{d}\right) \qquad (V.1)$$

Where,

$D$ : Packed bed column diameter (m)

$d$ : Particle diameter (m)

$\varepsilon_b$ : Average bed porosity at infinite column diameter

For randomly packed beds there are four considerable packing modes present: (a) very loose random packing ($\varepsilon_b \approx 0.44$) obtained by gradual de-fluidization of a fluidized bed or sedimentation; (b) loose random packing ($\varepsilon_b \approx 0.40$-$0.41$) obtained by letting spheres roll individually in place, or by dropping the spheres into the container as a loose mass; (c) poured random packing ($\varepsilon_b \approx 0.375$-$0.391$) obtained by pouring spheres into the container; and (d) dense random packing ($\varepsilon_b \approx 0.359$-$0.375$) obtained by vibrating or shaking down the packed bed (Rady, 2009).

The average bed to particle diameter in the present study is close to the value of 11 and using the value of $\varepsilon_b$ range given for poured random packing in (c) will be appropriate. By replacing the values to Eq. (V.1) the void fraction is calculated as **"ε=0.385"**.

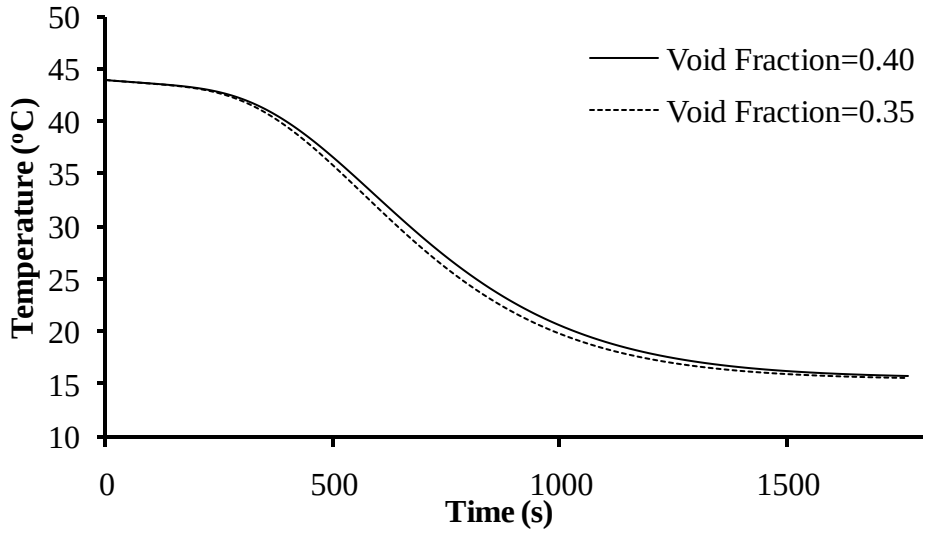


**Figure V.3 Model results showing the effect of void fraction on the outlet fluid temperature during a cooling simulation (Re=11.8, Flow rate=0.0078 L/s, $T_{in}$=15°C)**

Figure V.3 shows the effect of using limit values of void fraction in the present model for randomly packed beds. The present model was run for the given values of

void fraction and it is revealed that taken the value of void fraction between 0.40 and 0.35 for random packing is logical.

### V.1.5 Dynamic Behavior of the Mathematical Model

When Eq. (III.1) and Eq. (III.2) are run simultaneously on the software Matlab®, for different fluid velocities during cooling and heating processes the below figures are obtained. As it can be seen in figures V.4 and V.5 which are obtained from cooling simulations, bed entrances are cooled suddenly, though the exit of the bed are cooled slowly with respect to the entrance. The same behavior is expected from the experimental results. Especially, the experimental bed outlet temperature values will be our reference data while comparing experimental results for different fluid velocities. In figures V.4 and V.5, only the effect of the initial temperature and the flow rate were shown.

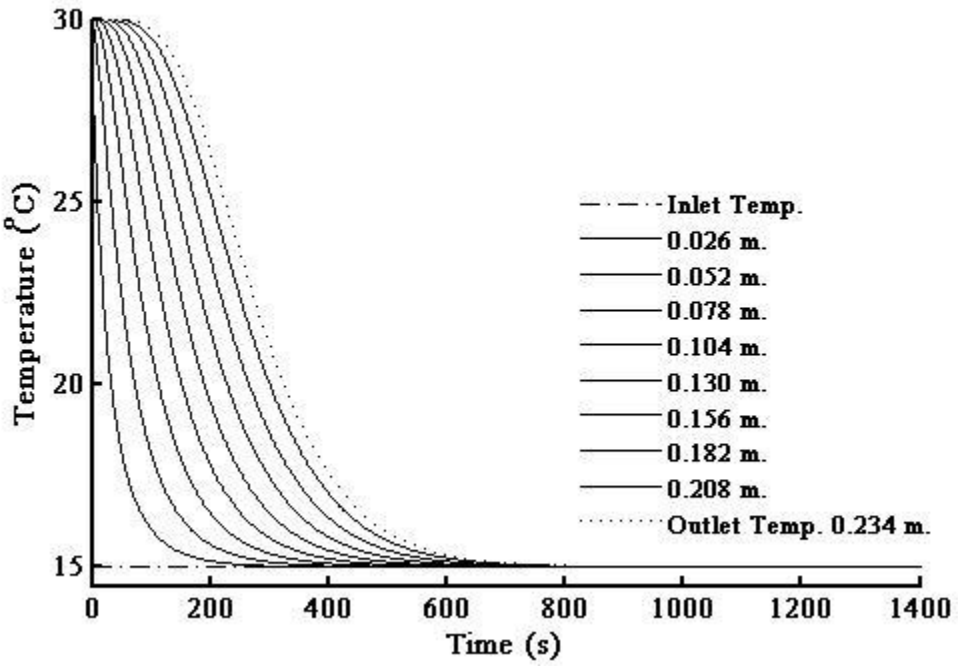


**Figure V.4 Temperature profiles across the packed bed for the simulation of a cooling experiment (Re=30.6, Flow rate=0.0202 L/s, $T_{in}$=15°C)**

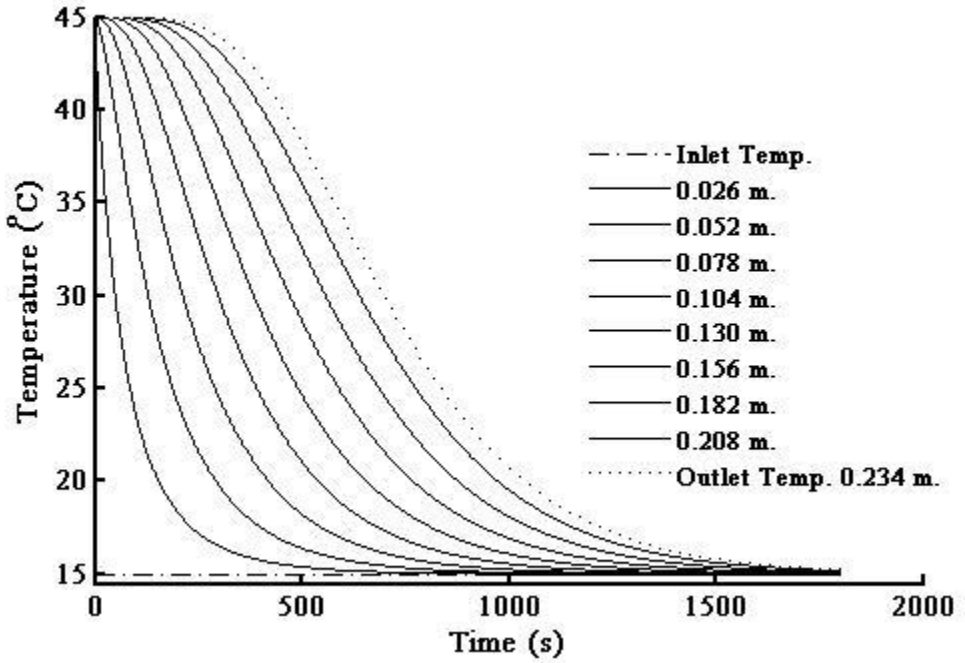


**Figure V.5 Temperature profiles across the packed bed for the simulation of a cooling experiment (Re=11.8, Flow rate=0.0078 L/s, $T_{in}$=15°C)**

Similar to the results of the cooling experiments, the temperature profiles obtained from the simulations for heating cycles were show by figures V.6 and V.7. The same behavior is observed that is to say the bed entrance temperature increases before the bed outlet temperature. However, in the experiments the packed bed outlet temperature will increase sharper than the model due to thermal mixing. The effect of the thermal mixing for cooling and heating experiments will be presented and discussed in sections V.2.4 and V.2.5.

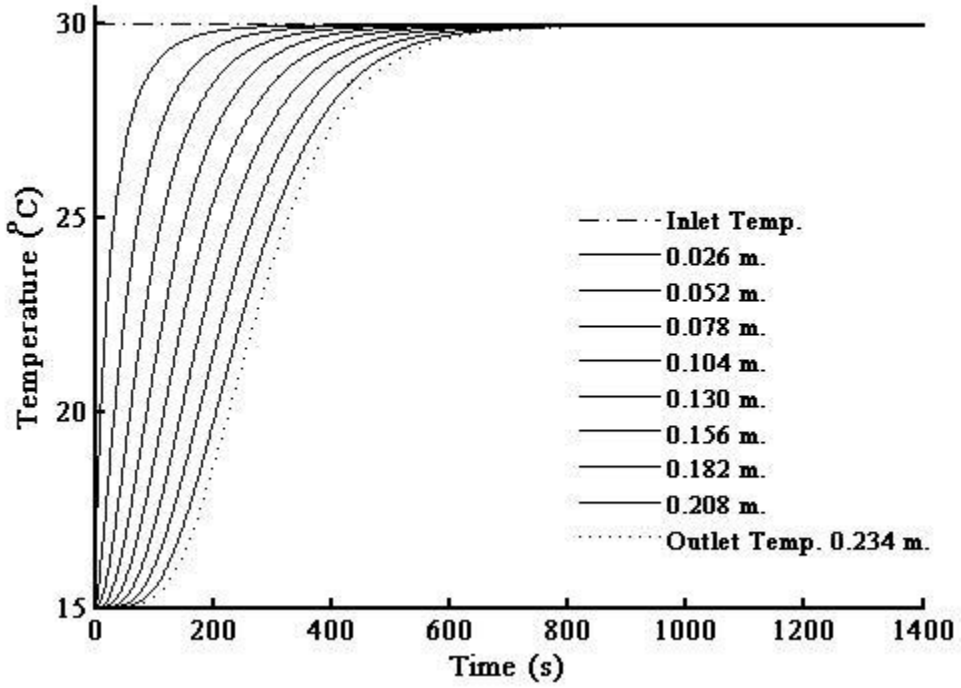


**Figure V.6 Temperature profiles across the packed bed for the simulation of a heating experiment (Re=43.5, Flow rate=0.0202 L/s, $T_{in}$=30ºC)**

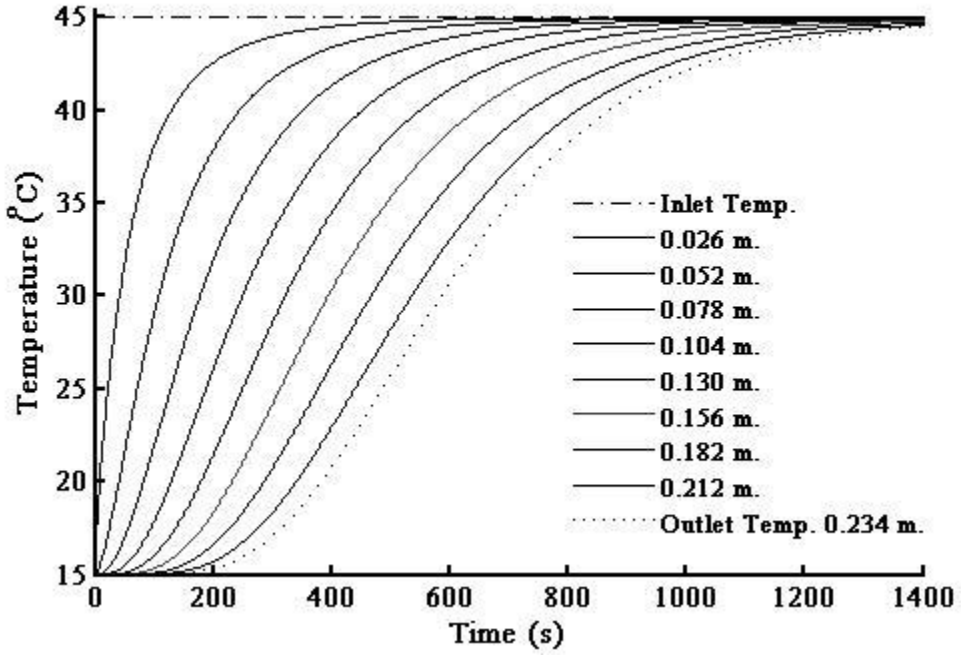


**Figure V.7 Temperature profiles across the packed bed for the simulation of a heating experiment (Re=27.0, Flow rate=0.0094 L/s, $T_{in}$=45ºC)**

### V.1.6 Comparison of Outlet Temperature Profiles of the Working Fluid and the Packing Material

As it was mentioned before, the model equations consist of both the variables of working fluid temperature $T$, and packing material temperature $T_s$. The model results which are given in Figure V.8 and V.9 were obtained using these two parameters, simultaneously. It is needed to say that the model was always run on the software including both of the two parameters. Although, the temperature profiles obtained from packed bed material are not shown in all figures to avoid any complication; however below figures V.8 and V.9 are exceptions.

It can be seen in the figures that the usage of the temperature profiles of the working fluid $T$, as the representative of the model results is logical. Since, there is no significant diversion between the temperature profiles of the working fluid and the packing material. To avoid any question marks for the reader, the model was run for cooling and heating cycles at different flow rates and temperature ranges.

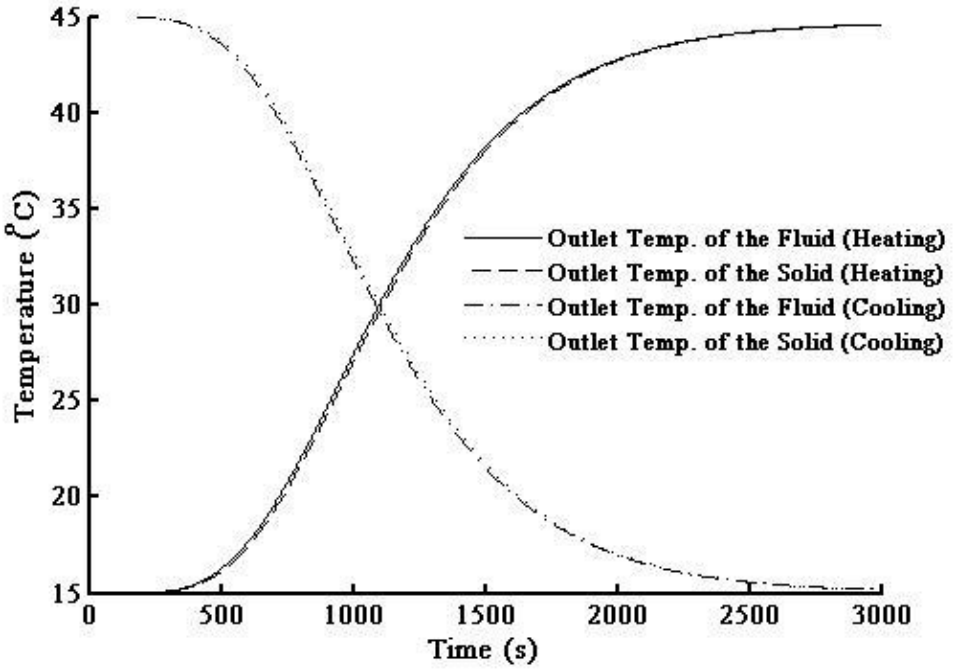


**Figure V.8 Temperature profiles comparison across the packed bed for the simulations of heating and cooling experiments (Flow rate=0.0050 L/s)**

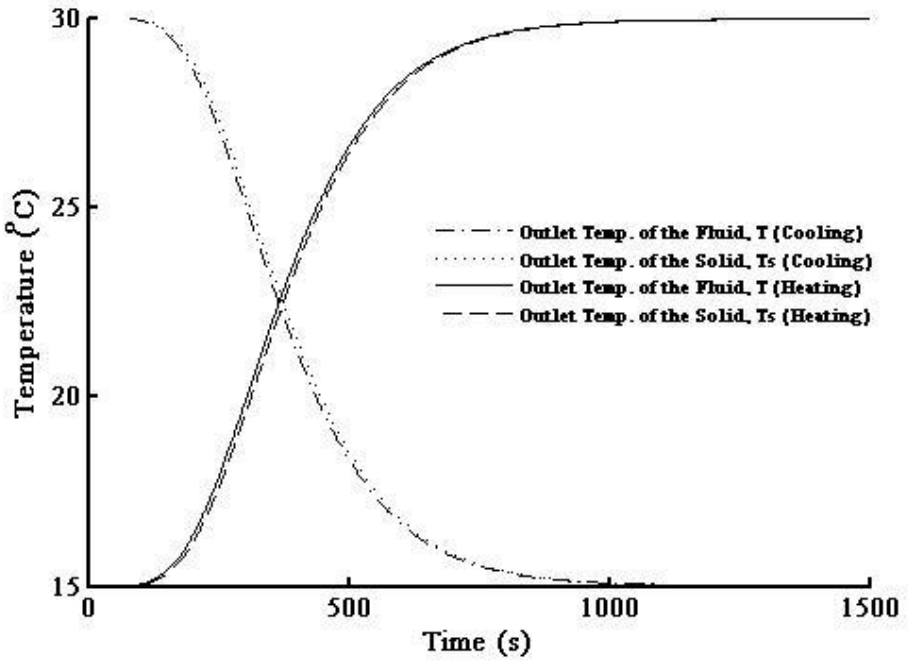


**Figure V.9 Temperature profiles comparison across the packed bed for the simulations of heating and cooling experiments (Flow rate=0.0150 L/s)**

## V.2 EFFECT OF FLUID VELOCITY AND TEMPERATURE RANGE

The fluid velocity affects the heating and cooling of the packed bed in three ways. First it appears in the advection equation as a multiplier and secondly it affects the convective heat transfer coefficient *h*, which is computed using the correlation given for the Nusselt number. As it was mentioned previously the Nusselt number is a function of both the Reynolds and Prandtl numbers. Additionally, the fluid velocity term appears in the correlation used to calculate the dispersion coefficient which was explained in Chapter II. Temperature range contributes especially the thermal mixing along the packed bed during heating cycles. Its effects are more influential at early stages, particularly during heating cycle. The effect of the thermal dispersion coefficient on the dynamic behavior of the packed bed will be explained in the coming sections.

### V.2.1 Influence of Fluid Velocity and Temperature Range during Heating and Cooling Experiments

Experimentally measured bed exit temperatures for different inlet temperatures and flow rates are shown in Figure V.10. In those curves it can be clearly seen that the slope of the curves at the very beginning of the experiments are functions of the

temperature difference between the entrance and exit temperatures. Natural convection is dominant at the initial stages of the experiments. As the heating progresses, the temperature difference decreases and the heat transfer mainly occurs with forced convection between the flowing water and glass beads in addition to the bulk flow in the axial direction.

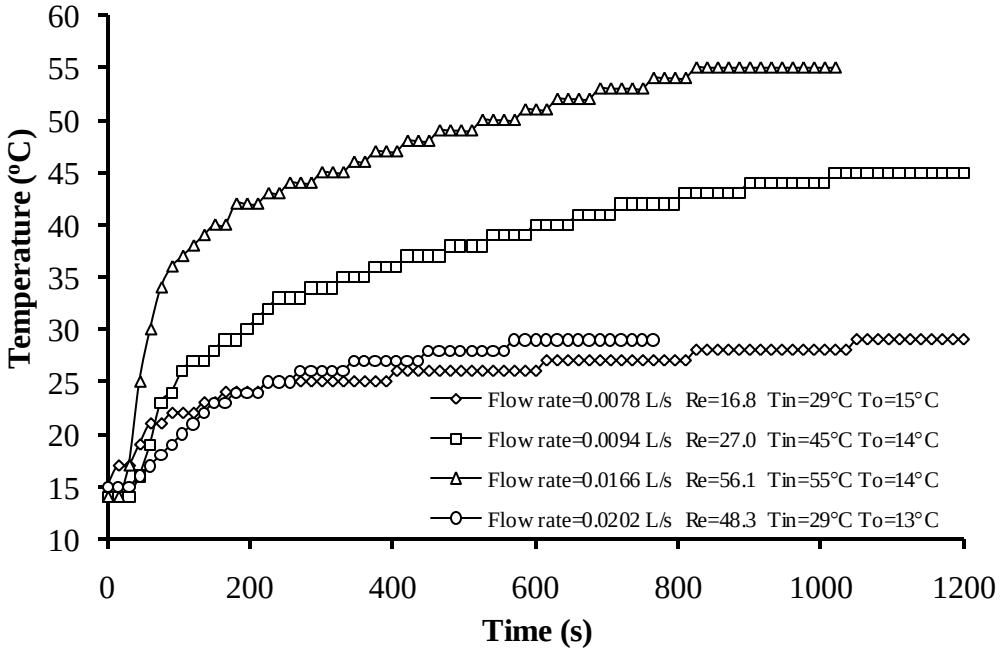


**Figure V.10 Packed bed outlet temperature for different heating experiments performed at different inlet temperatures and flow rates**

When the measured temperature profiles of the cooling experiments are plotted, it can be easily observed from Figure V.11 that due to the absence of any buoyancy forces –a fluid with lower density goes up, $\rho(T)$- there is no disturbing thermal mixing during cooling. It is seen that the factor determines the behavior of the temperature profiles is fluid velocity (Reynolds number). Since, there is no significant velocity difference between two cooling experiments from 55ºC to 15ºC total cooling times of both experiments are nearly the same. The same behavior is observed even when there are separate initial temperatures such as 45ºC and 30ºC for which the durations of the cooling experiments remained the same due to the equal fluid velocities (Reynolds numbers).

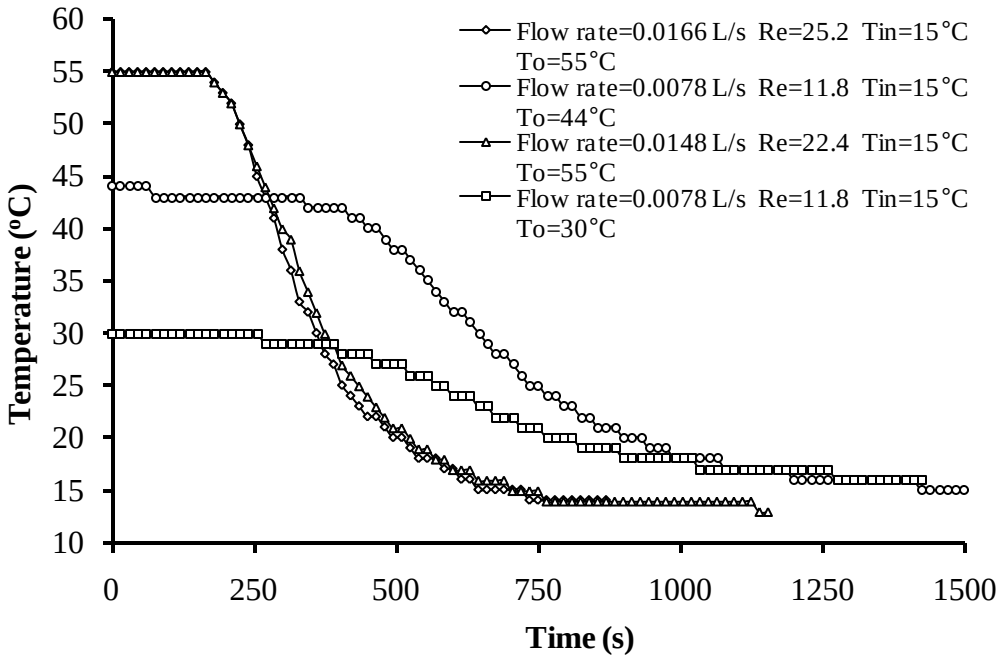


**Figure V.11 Packed bed outlet temperature for different cooling experiments performed at different inlet temperatures and flow rates**

### V.2.2 Comparisons of the Model and the Experimental Results for Heating and Cooling Cycles

Temperature profiles obtained from the simulations using the model, and experimental measurements at the packed bed exit were shown in figures V.12 and V.13 for two heating experiments. Due to natural convection sudden rise in the measured bed exit temperature is observed. This is the phenomenon of thermal dispersion or thermal mixing which is observed when the fluid inlet temperature at the bottom of the bed is higher than the initial temperature of the bed. At the beginning of the experiment there is a large temperature difference between the top and bottom of the packed bed. As heating progresses the temperature difference decreases and thus the effect of the thermal mixing diminishes. Therefore simulated temperature profiles at different levels of the packed bed are plotted together with the experimentally measured bed exit temperature. Temperature range contributes especially the thermal mixing along the packed bed. Its effects are more influential at early stages, particularly during heating processes. In this section, the results for two heating and two cooling experiments were presented. Other experimental and simulation results are presented in Appendix E.

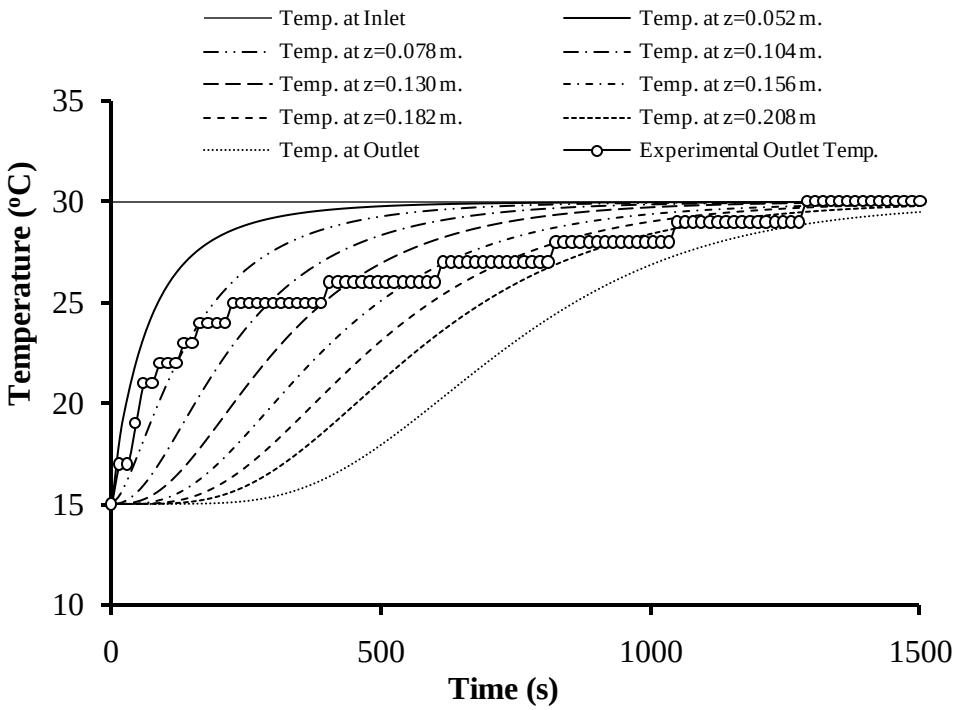


**Figure V.12 Temperature profiles across the packed bed for the simulation of a heating experiment together with heating experimental results (Re=16.8, Flow rate=0.0078 L/s, $T_{in}$=30ºC)**

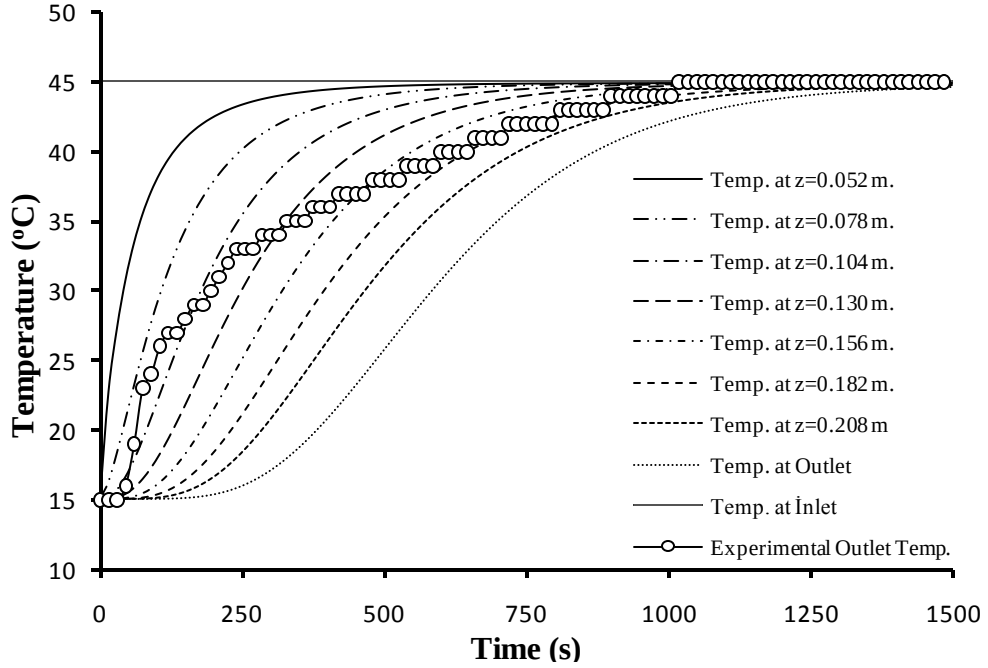


**Figure V.13 Temperature profiles across the packed bed for the simulation of a heating experiment together with heating experimental results (Re=27, Flow rate=0.0094 L/s, $T_{in}$=45ºC)**

The model results and measured temperatures show a satisfactory agreement for cooling experiments shown by figures V.14 and V.15. Figure V.14, represents the model and experimental results for a cooling cycle from 29 to 15°C. In this experiment, the thermocouple is placed at the middle of the packed bed. In all other heating and cooling experiments (four heating and four cooling experiments), the movable thermocouple is placed right at the top of the packed bed to measure the experimental outlet temperature. The close agreement between the model and experimental results is a good indication of the absence of thermal mixing due to the flow of the cold inlet stream from the bottom to the top of the packed bed. The model results were obtained without considering the effect of the thermal mixing.

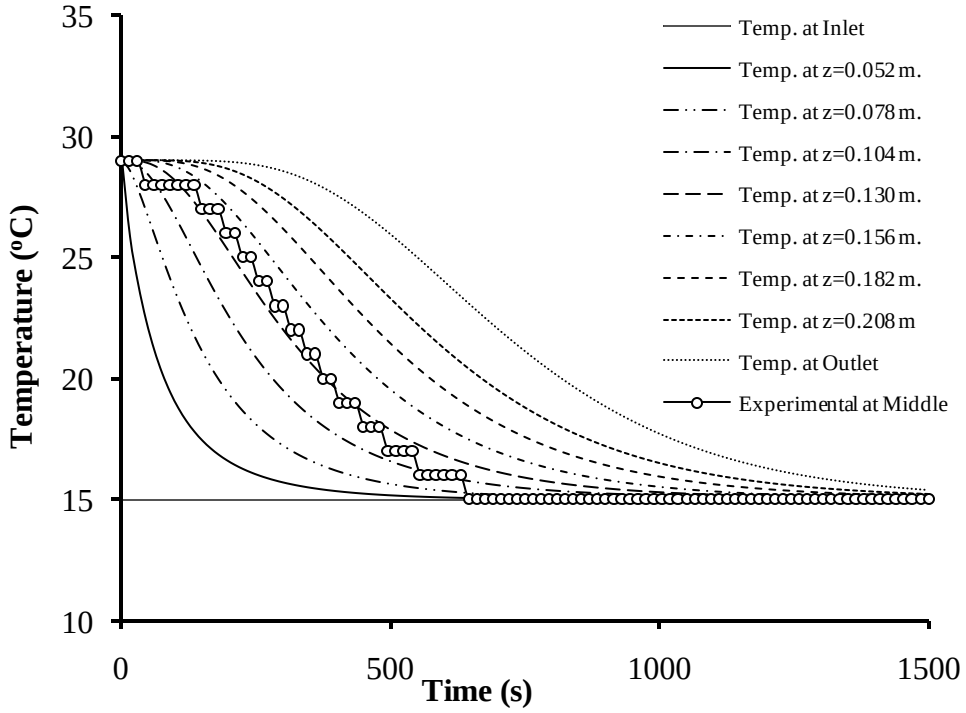


**Figure V.14 Temperature profiles across the packed bed for the simulation of a cooling experiment together with cooling experimental results (Re=11.8, Flow rate=0.0078 L/s, $T_{in}$=15°C)**

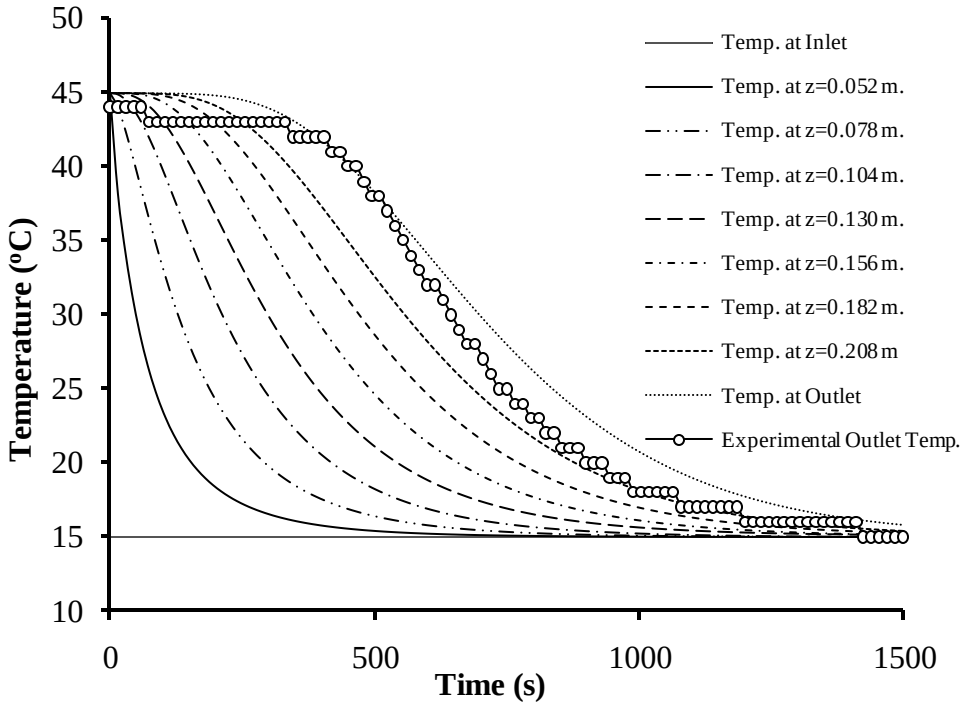


**Figure V.15 Temperature profiles across the packed bed for the simulation of a cooling experiment together with cooling experimental results (Re=11.8, Flow rate=0.0078 L/s, $T_{in}$=15ºC)**

### V.2.3 Dimensionless Temperature versus Dimensionless Time for Heating and Cooling Experiments

In the following pages, packed bed exit temperature profiles for different experimental runs will be presented using dimensionless temperature $\boldsymbol{\theta}$ and dimensionless time $\boldsymbol{\tau}$, as variables. Dimensionless time $\boldsymbol{\tau}$ is referred as the ratio of the volume flow rate multiplied by time to the void volume of the packed bed. Dimensionless temperature $\theta$ means the ratio of temperature difference between the measured exit temperature and initial temperature to the difference between the inlet and initial temperatures. Calculation of dimensionless time and dimensionless temperature is shown in Eq. (V.2) and Eq. (V.3) respectively.

$$\tau = \frac{Vt}{\varepsilon V} \tag{V.2}$$

$$\theta = \frac{T(t) - T_0}{T_{in} - T_0} \tag{V.3}$$

When dimensionless temperatures versus dimensionless time curves are plotted for cooling experiments in Figure V.16, it can be seen that all four experiments behave the same. Significant decrease in the dimensionless temperature is observed when the dimensionless time reaches to the value of 1 and cooling continues until the dimensionless time reaches approximately a value between 3.5 and 4. These results show that the fitting of the model parameters such as the Nusselt number correlation and thermal dispersion coefficient for any experiment will tune the model for all cooling experiments.

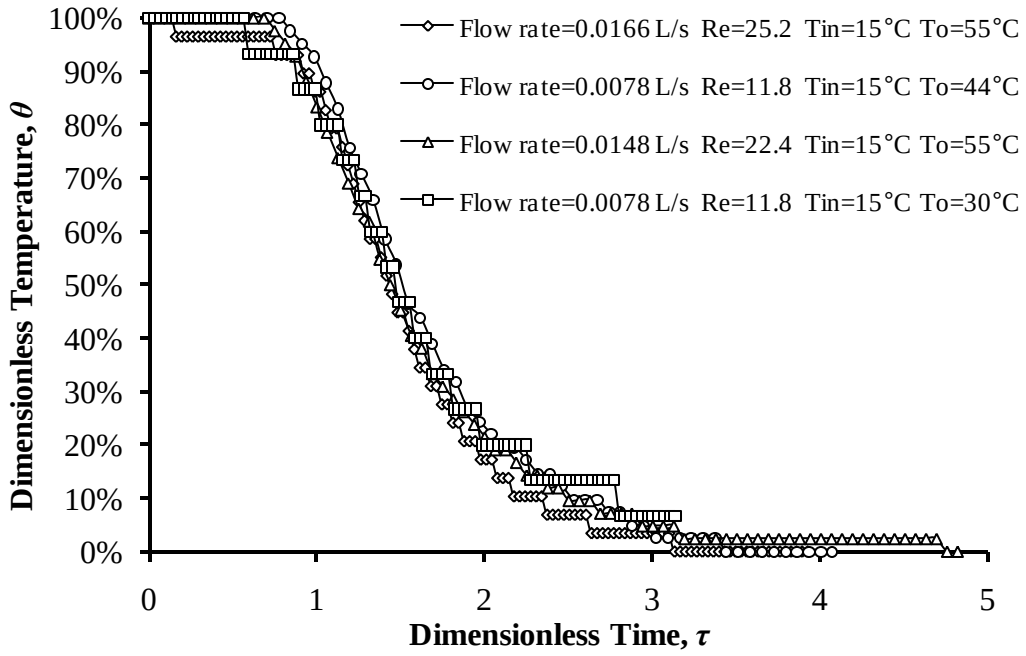


**Figure V.16 Dimensionless temperature versus dimensionless time curves for different cooling experiments**

Similar to the cooling experiments, the dimensionless temperatures for different heating experiments was plotted versus dimensionless time in Figure V.17. For the heating experiments, dimensionless temperature profiles differ slightly depending on the flow rate or in other words on the Reynolds number and the difference between the fluid inlet and initial temperatures. Around a value of dimensionless temperature between 75 and 85% and a value of dimensionless time between 1.5 and 2.0 the slopes of the curves change significantly. Similar to the cooling experiments heating of the packed bed is completed when dimensionless time reaches to a value around 4.0. The effect of the Reynolds number after a value

of dimensionless time of 1.5 is clearly visible. In Figure V.17, the four experiments can be grouped into two. One of these two groups is the experiments performed for Reynolds numbers 16.8 and 27.0 for two different inlet temperatures such as 29 and 45°C. The other group is the two experiments performed at Reynolds numbers 48.3 and 56.1. The effect of the thermal dispersion diminishes and the heat transferred to the upper levels of the packed bed is predominantly with the bulk flow after a value of the dimensionless time of 1.5. Before this value thermal dispersion is the dominant mechanism for the heat transfer along the packed bed (from bottom to the top) since the temperature difference is higher at the initial stages of the heating cycles.

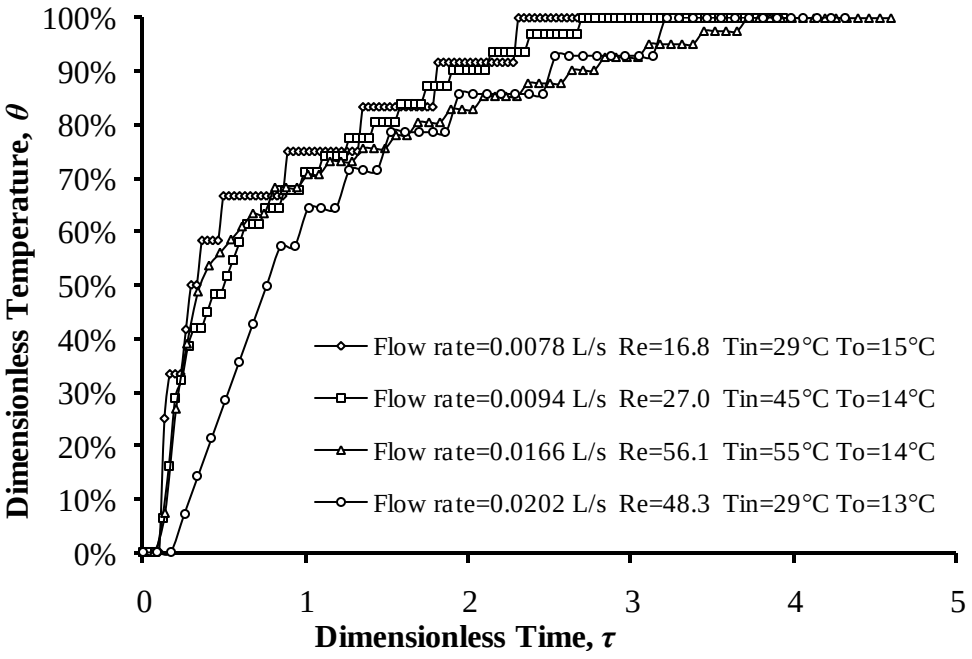


**Figure V.17 Dimensionless temperature versus dimensionless time curves for different heating experiments**

### V.2.4 Effect of the Thermal Dispersion Coefficient on the Dynamic Behavior during Cooling

Thermal behavior of the packed bed gives an idea about which axial dispersion coefficient correlation should be used. A comparison of the experimental results and the axial dispersion coefficient correlations of Wakao, (1979) and Aris-Taylor taken from Fogler, (2005) is made in figures V.18 and V.19 during cooling process. Since, there is no buoyancy forces affecting the thermal behavior of the bed during cooling,

using the results of two of the cooling experiments is a logical approach to determine the correlation to be used. As it is seen in figures V.18 and V.19 the correlation of Wakao, (1979) is in a very good agreement with the experimental results. However, the disagreement of Aris-Taylor correlation is quite obvious.

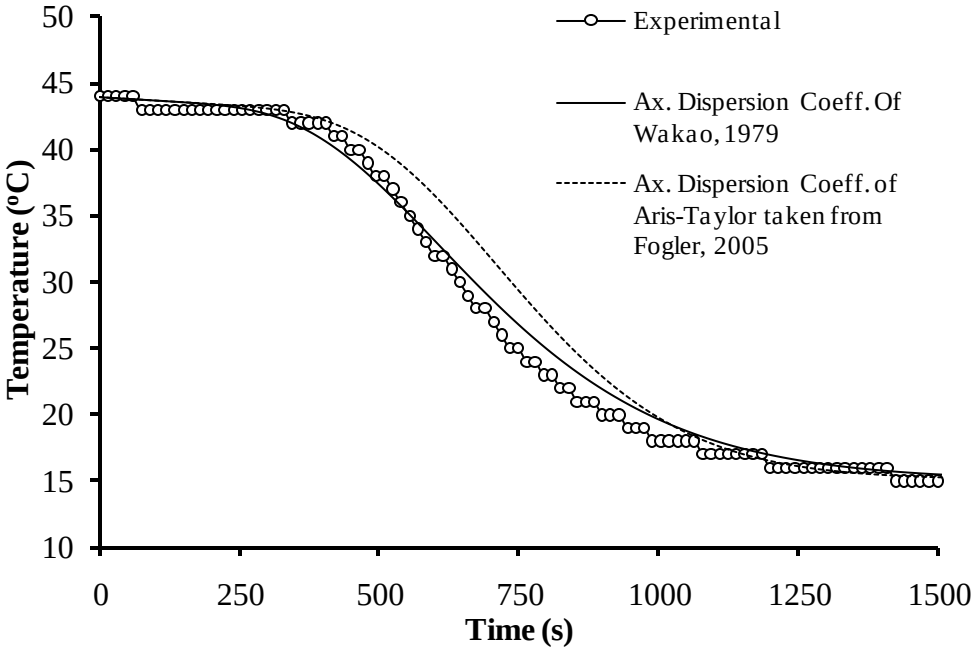


**Figure V.18 Comparison of axial dispersion coefficient correlations to simulate the packed bed outlet temperature during a cooling experiment (Re=11.8, Flow rate of 0.0078 L/s, $T_{in}$=15ºC)**

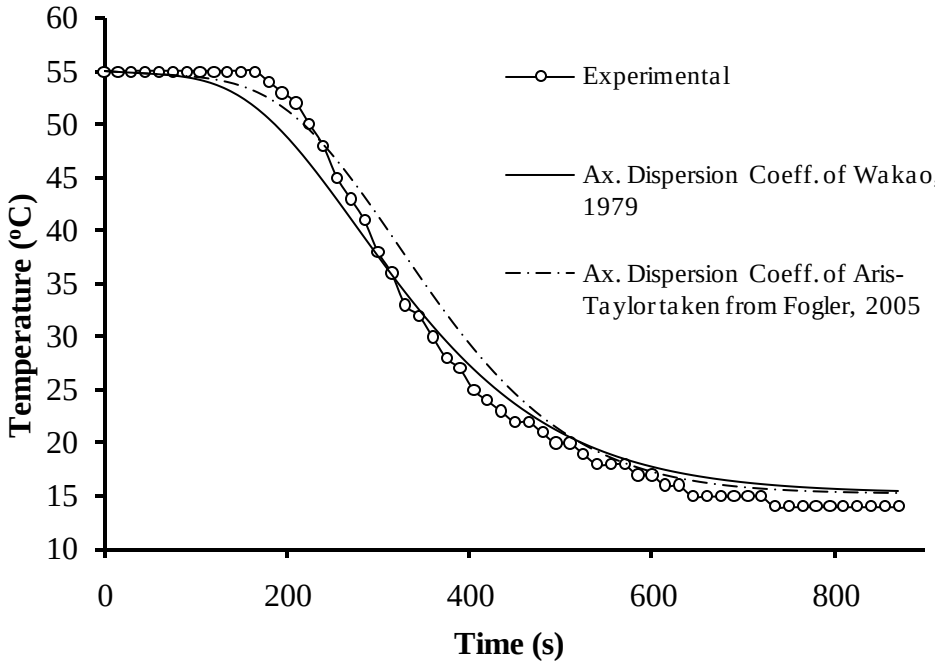


**Figure V.19 Comparison of axial dispersion coefficient correlations to simulate the packed bed outlet temperature during a cooling experiment (Re=25.2, Flow rate of 0.0166 L/s, $T_{in}$=15°C)**

### V.2.5 Effect of the Thermal Dispersion Coefficient on the Dynamic Behavior during Heating

Heating experiments have been very inspiring throughout the discussion chapter of this study because of its contribution to develop an accurate axial thermal dispersion coefficient for the model. At the initial stages of a heating cycle, there is a considerable temperature difference between water as the working fluid and the packed bed. This temperature difference causes to form buoyancy forces -*a fluid with lower density goes up*- due to the location of the pipe entrance. As a result of the buoyancy forces thermal mixing (dispersion) occurs, especially at the initial stages. It can be stated that, the influence of axial dispersion coefficient $k_d$ becomes more pronounced when the temperature difference is high, and thus the correlation to include the effect of thermal mixing should be multiplied with a convenient value for heating experiments.

Figures V.20 and V.21 show the behavior of the present model using multiplied $k_d$ values. They show that the thermal mixing diminishes in time due to decreasing of temperature difference between the inlet and outlet of the bed. Using the obtained results given in figures V.20 and V.21, it can be easily revealed that

multiplying the axial thermal dispersion coefficient by 15 makes the model applicable at finishing stage of heating. However, using the value of 40 as a multiplier makes the results agreeable at the initial stage of heating. Unfortunately, there is no related work published in the literature analyzing and bringing a clear understanding to the thermal mixing phenomena due to buoyancy forces resulting from the temperature difference.

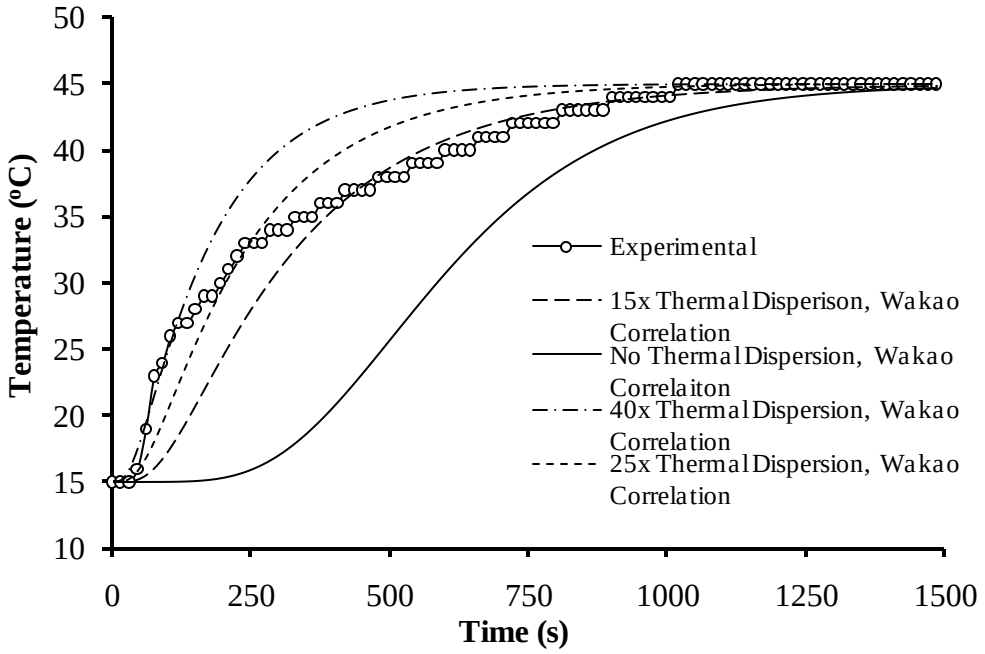


**Figure V.20 Thermal behavior of the bed during heating (Flow rate=0.0094 L/s, Re=22.4, $T_{in}$=45ºC)**

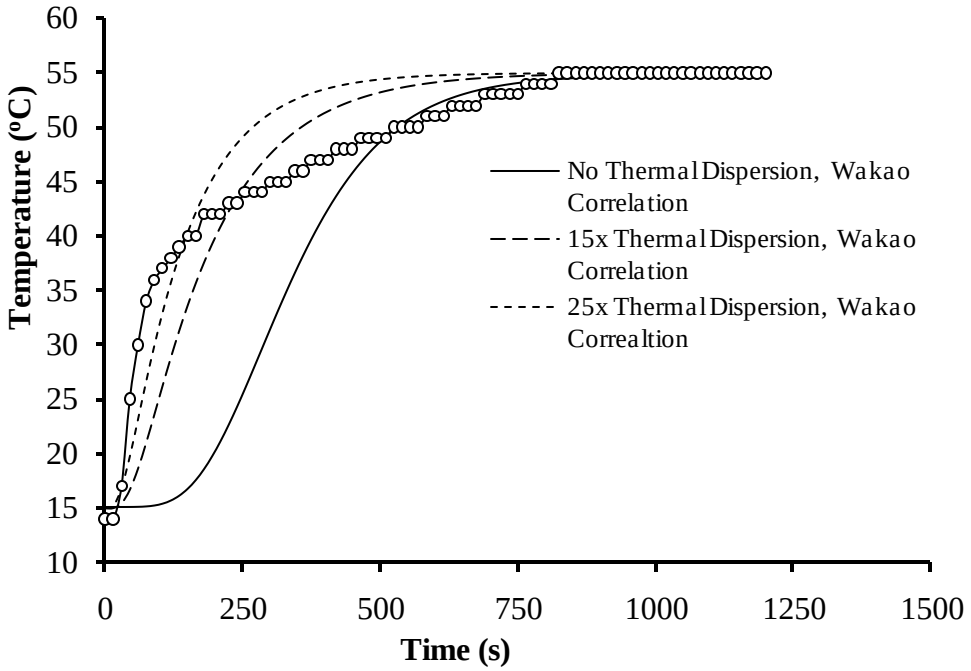


**Figure V.21 Thermal behavior of the bed during heating (Flow rate=0.0166 L/s, Re=56.1, $T_{in}$=55°C)**

### V.2.6 Analysis of Dynamic Behavior of the Bed with Dimensionless Numbers

In the study of Pu et al. (1999) it was shown that the values of *Ra/Pe* determines the type of the flow regime. The physical meaning of Peclet number *Pe* can be described as the ratio of the rate of advection of a physical quantity by the flow to the rate of diffusion of the same quantity driven by an appropriate gradient.

$$Pe = RePr \qquad (V.4)$$

The cause of thermal mixing includes both the effects of advection and buoyancy forces. Peclet number is used for its representation of the rate of advection through the bed. On the other hand Rayleigh number is related with temperature range and buoyancy forces; therefore, it represents the behavior of the bed when such forces are present. The physical meaning of Rayleigh number *Ra* can be viewed as the ratio of buoyancy forces and (the product of) thermal and momentum diffusivities.

$$Ra = \frac{g\beta K\Delta T D_{tank}}{\upsilon \alpha_m} \qquad (V.5)$$

In the case of *Ra/Pe*<1, the forced convection is predominate. On the other hand, when 1<*Ra/Pe*<105, the mixed convection flow regime is present. Table V.1 lists the values of the dimensionless groups which are calculated using the experimental results. It can be seen that the effect of the natural convection and thus the mixed convection appears for heating experiments performed at Reynolds numbers 27.0 and 56.1 for which *Ra/Pe* ratios are 1.39 and 1.88, respectively.

**Table V.1 Values of dimensionless groups calculated using experimental results**

| Flow Rate (L/s) | Temperature Range (°C) | The Process | *Re* | *Pr* | *Pe* | *Ra* | *Ra/Pe* |
|---|---|---|---|---|---|---|---|
| 0.0078 | 15-30 | Heating | 16.8 | 5.43 | 91.2 | 50.6 | 0.55 |
| 0.0202 | 15-30 | Heating | 48.3 | 5.43 | 262.3 | 50.6 | 0.19 |
| 0.0094 | 15-45 | Heating | 27.0 | 4.95 | 133.6 | 187 | 1.39 |
| 0.0166 | 15-55 | Heating | 56.1 | 3.28 | 184.0 | 346 | 1.88 |
| 0.0166 | 55-15 | Cooling | 25.2 | 8.25 | 207.9 | 47 | 0.23 |
| 0.0078 | 44-15 | Cooling | 11.8 | 8.25 | 97.3 | 35 | 0.36 |
| 0.0148 | 55-15 | Cooling | 22.4 | 8.25 | 184.8 | 47 | 0.25 |
| 0.0078 | 30-15 | Cooling | 11.8 | 8.25 | 97.3 | 17.5 | 0.18 |

The above results tell that the packed bed system used in this work includes both heat transfer mechanisms of forced convection and natural convection (causes thermal mixing) at the same time throughout the experiments. However, calculation of Rayleigh number does not include the parameter of fluid velocity which has a great effect on thermal mixing in the present study.

## V.3 OPTIMIZATION

Optimizing the PBHS unit includes examining the behaviors of various parameters such as durations of heating and cooling cycles, type of the used packing material, length of the packed bed and working fluid flow rate. The most significant parameter to optimize the system is durations of cooling and heating cycles, thus the dimensionless time $\tau$. All of the investigations for optimizing the PBHS unit were performed with respect to dimensionless time $\tau$.

### V.3.1 Effect of the Packing Material Properties on the Dynamic Behavior of the Packed Bed Heat Storage Unit

The model was simulated for heating and cooling cycles of the bed using the physical properties of glass and steel beads, separately, to investigate the effect of the

packing material on the dynamic behavior of the PBHS unit. During these simulations, the properties of the packing materials given in Table V.2 were used.

**Table V.2 Physical properties of the packing material (Steel and Glass beads) used for the optimization of the PBHS unit**

| | $\rho$ (kg/m$^3$) | $C$ (kJ/kg°C) | $k$ (J/ms°C) | **Diameter** (m) |
|---|---|---|---|---|
| **Steel Beads** | 7820 | 0.490 | 16 | 0.0260 |
| **Glass Beads** | 2400 | 0.840 | 0.96 | 0.0260 |

Figure V.22 and V.23 show the dynamic thermal behavior of the packing materials, during cooling and heating cycles. As it is seen in Figure V.22, the bed packed with glass beads is cooled faster than the bed packed with steel beads. When Figure V.22 is compared to Figure V.23, during cooling cycle the elapsed time until the end of cycle is longer. The comparison of obtained dimensionless time values at the end of cooling and heating was made using Table V.3. The table is constructed using the values taken from cooling and heating simulations which are plotted in figures V.22 and V.23. It was observed that the steel beads as packing material has greater dimensionless time value 6.35, comparing the value of the packing material of glass beads 4.50 at the end of cooling cycle. Similar to the cooling cycle, at the end of heating cycle, the steel beads as packing material has greater dimensionless time value 5.24, comparing the value of the packing material of glass beads 3.70.

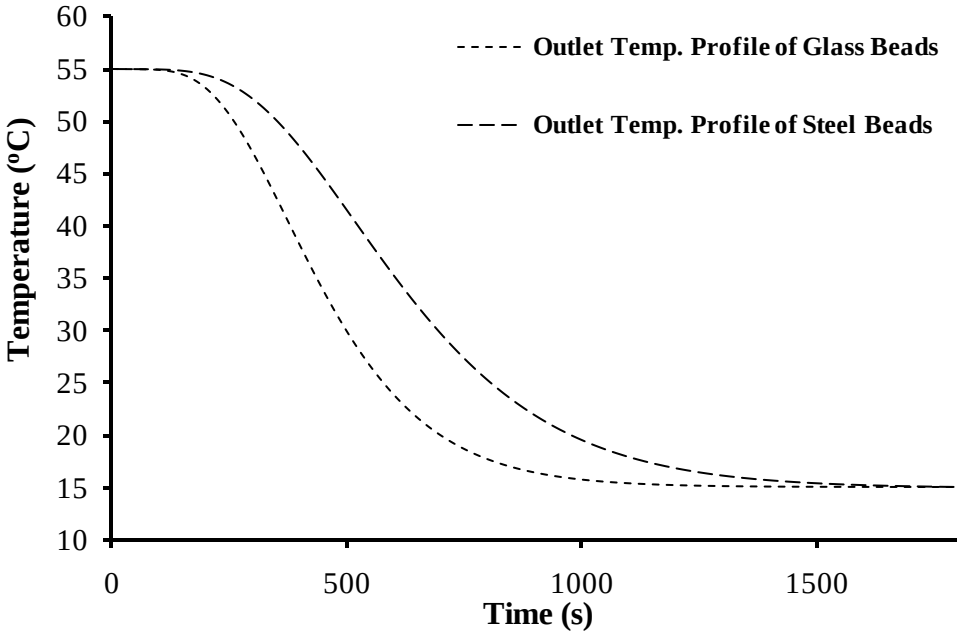


**Figure V.22 Outlet temperature profiles across the packed bed for the simulation of a cooling experiment for different packing material (Re=19, Flow rate=0.0125 L/s, $T_{in}$=15°C, $T_0$=55°C)**

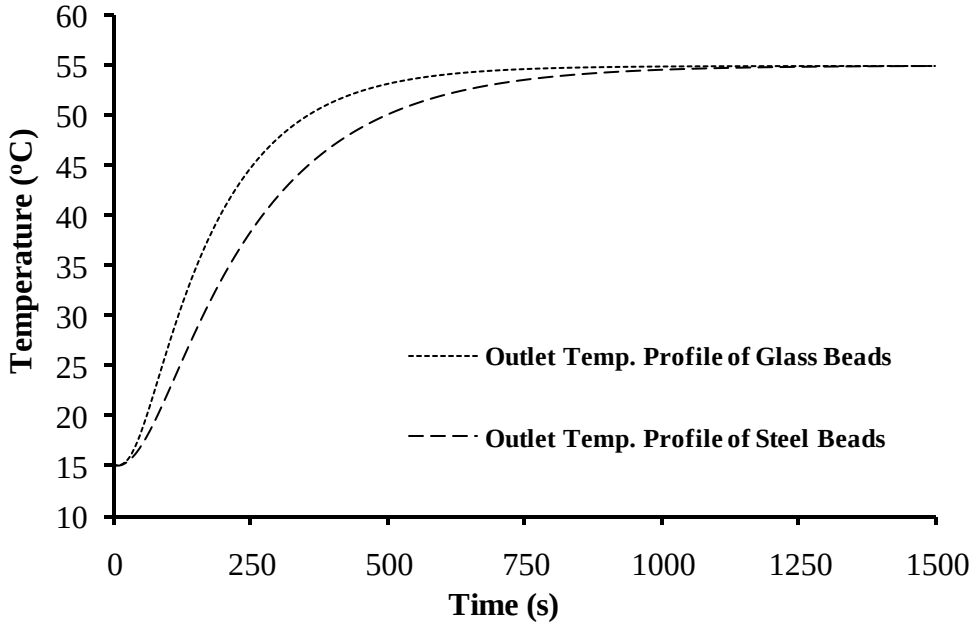


**Figure V.23 Outlet temperature profiles across the packed bed for the simulation of a heating experiment for different packing material (Re=42.3, Flow rate=0.0125 L/s, $T_{in}$=55°C, $T_0$=15°C, $k_d$x25)**

From these observations, it is concluded that using steel beads as the packing material will be the right choice, since greater dimensionless time values are obtained during both cooling and heating cycles.

**Table V.3 Dynamic behavior of the packing material (Steel and Glass beads) used for the optimization of the PBHS unit**

| | Reached Temp. at the end of Cooling (°C) | Reached Temp. at the end of Heating (°C) | Value of τ (cooling) | Value of τ (heating) |
|---|---|---|---|---|
| **Steel Beads** | 15.12 | 54.90 | 6.35 | 5.24 |
| **Glass Beads** | 15.12 | 54.90 | 4.50 | 3.70 |

### V.3.2 Effect of the Working Fluid Flow Rate and the Packed Bed Length on the Dynamic Behavior of the Packed Bed Heat Storage Unit

After determining the optimum (practical) type of the packing material as steel beads, the next step is to determine the optimum packed bed length and working fluid flow rate. Evaluating a few simulations using different bed lengths and flow rates, the most beneficial simulation results are shown in figures V.24 and V.25 for cooling and heating cycles. The purpose of these simulations is to obtain the dimensionless time values at the end of each performed simulation. It is found convenient to take six different constraints for each cooling and heating cycles. The plotted temperature profiles are representing outlet temperatures of the PBHS unit. During these simulations the diameter of the PBHS unit is taken constant as it is real diameter of the experimental setup used for this thesis. Additionally, the model does not include any term representing radial dynamic behavior of the packed bed.

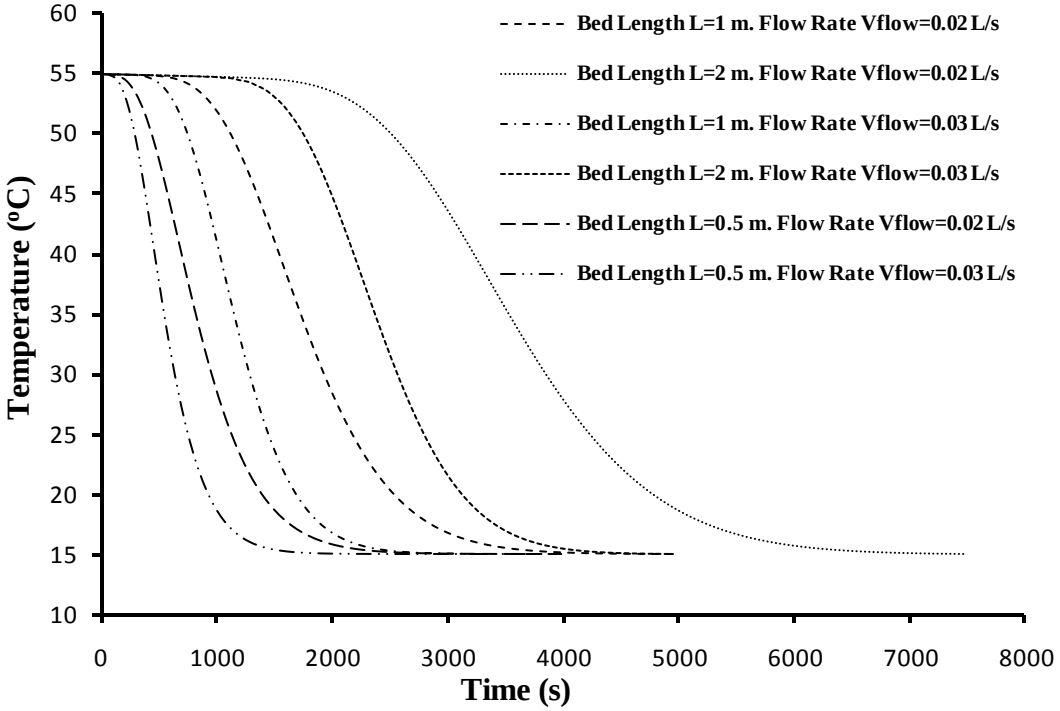


**Figure V.24 Outlet temperature profiles across the packed bed for the simulation of cooling cycles for different bed lengths and flow rates using steel beads as packing material**

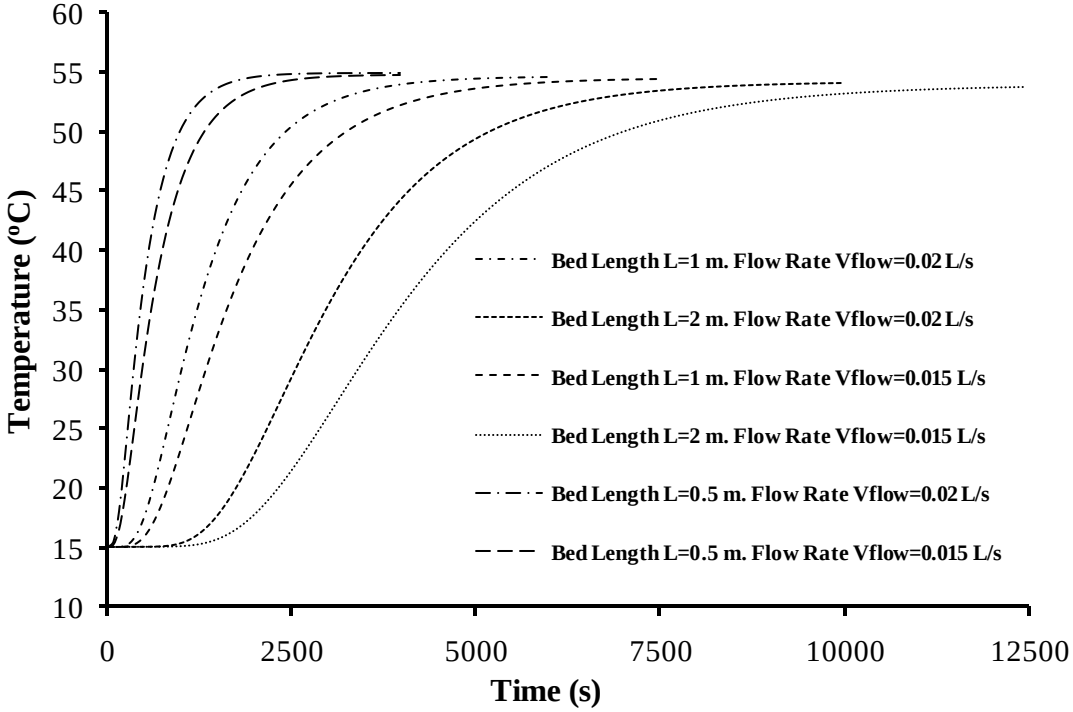


**Figure V.25 Outlet temperature profiles across the packed bed for the simulation of heating cycles for different bed lengths and flow rates using steel beads as packing material**

The dimensionless time values obtained from the simulations of cooling and heating cycles for different packed bed length and working fluid flow rates were calculated when the desired temperature was reached. The desired temperatures are taken as 15.1ºC for cooling simulation and 54.5ºC for heating simulation. The corresponding calculations are tabulated in Table V.4.

**Table V.4 Dimensionless time values obtained by simulating the model for various bed lengths and flow rates during cooling and heating cycles**

| | **L=1.0 $V_{flow}$=0.02** | **L=2.0 $V_{flow}$=0.02** | **L=1.0 $V_{flow}$=0.03** | **L=2.0 $V_{flow}$=0.03** | **L=0.5 $V_{flow}$=0.02** | **L=0.5 $V_{flow}$=0.03** |
|---|---|---|---|---|---|---|
| **Reached τ Value at the end of Cooling** | 5.89 | 4.99 | 5.69 | 4.87 | 7.19 | 7.19 |
| | **L=1.0 $V_{flow}$=0.02** | **L=2.0 $V_{flow}$=0.02** | **L=1.0 $V_{flow}$=0.015** | **L=2.0 $V_{flow}$=0.015** | **L=0.5 $V_{flow}$=0.02** | **L=0.5 $V_{flow}$=0.015** |
| **Reached τ Value at the end of Heating** | 6.79 | <6.64 | 7.49 | <6.21 | 5.39 | 5.24 |

As a design parameter, the dimensionless time determines the duration of the heating or cooling in addition to the volume of the packed bed and the flow rate. The higher the $\rho C_p$ value of the material is the higher the dimensionless time. Once the desired duration of heating and cooling determined, then the volume of the packed bed can be designed for a range of working fluid flow rate.

# CHAPTER VI

## CONCLUSION

Packed beds are extensively used in the chemical and process industries as reactors, separators, dryers, filters and heat exchangers. Heat transfer can play a crucial role determining the performance of such devices. Therefore, it is taken as the subject of this thesis. The aim of this work was decided as the investigation of temperature distribution profiles of packed bed heat storage (PBHS) tank for developing a mathematical model.

The foundation of the model relates itself to the phenomena of one-dimensional heat transfer equation. The model is widely used in literature for different kinds of packed bed systems and it was found very convenient for the PBHS system that was used in this study. It includes all the necessary concepts of heat transfer mechanisms that take place in the used PBHS system. To be able to represent the PBHS unit completely, the model was adjusted. The adjusted model used in this study includes particular modifications of the model due to the specific assumptions for simplifying the present PBHS unit. The purpose of simplifying assumptions was to reduce the number of parameters and the number of variables appearing in the model equations.

Despite working with limited tools, this thesis suggests a logical approach on thermal mixing phenomena that is encountered due to buoyancy forces during heating. It was revealed by this work that thermal mixing can be represented in the model by using the suitable thermal dispersion coefficient correlation and multiplying the coefficient by a value between 15 and 30. **Unfortunately, there is no related work published in the literature analyzing and bringing a clear understanding to the thermal mixing phenomena due to buoyancy forces resulting from the temperature difference.**

Dimensionless time as used to define the completion of heating and cooling cycles. The range of dimensionless time was determined for different packing materials, bed length and working fluid flow rate. It was shown that the optimal design of the packed bed is possible by using the mathematical model results.

# REFERENCES


Ali Jalalzadeh-Azar, A.: Glenn Steele, W.: George Adebiyi, A.: "Performance comparison of high-temperature packed bed operation with PCM and sensible-heat pellets" International Journal of Energy Research, 21 **(1997)** 1039-1052.

Altuntop, N.: Kilik, Z.: Ozceyhan, V.: Kincay, O.: "Effect of water inlet velocity on thermal stratification in a mantled hot water storage tank" International Journal of Energy Research, 30 **(2006)** 163-176.

Beasley, D. E.: Clark, A. J.: "Transient response of a packed bed for thermal energy storage" International Journal Heat and Mass Transfer, 27 **(1984)** 1659-1669.

Bıyıkoglu, A.: "Optimization of a sensible heat cascade energy storage by lumped model", Energy Conversion and Management, 43 **(2002)** 617-637.

Dincer, İ.: Dost, S.: Li, X.: "Performance analyses of sensible heat storage systems for thermal applications" International Journal of Energy Research, 21 **(1997)** 1157-1171.

Fogler, H.S.: *Elements of Chemical Reaction Engineering,* Prentice Hall International New York, USA, **(2005)** 966.

Galloway, T. R.: Sage, H.: "A model of mechanism of transport in packed, distended and fluidized beds" Chemical Engineering Science, 25 **(1970)** 495-506.

Gunn, D.J.: "Transfer of heat and mass to particles in fixed and fluidized beds" International Journal of Heat and Mass Transfer, 21 **(1978)** 467-476

Hanrattry, T. J.: "Nature of wall heat transfer in packed beds" Chemical Engineering Science, 3 **(1954)** 209-214.

Holman,J.P.: "Heat Transfer", 5 th Edition; McGraw-Hill Inc., Tokyo, JAPAN, **(1983)** 2-6 and 168-172.

Geankoplis, C.J.:"Transport Processes and Separation Process Principles", 4 th Edition; Pearson Education, U.S.A., **(2007).**

Huynh, B.P.: "Free convection cooling of a horizontal cylinder positioned above a plane" Proc. 13$^{th}$ International Heat Transfer Conference, Sidney, Australia, **13-18/08/2006**.

Karahan, H.: “Solution of weighted finite difference techniques with Advection-Diffusion Equation using Spreadsheets” Computer Applications in Engineering Education, 16 **(2008)** 147-156.

Klerk, A.: “Voidage variation in packed beds at small column to particle diameter ratio” AIChE Journal, 49 **(2003)** 2022-2029.

Pu, W. L.: “An experimental study of mixed convection heat transfer in vertical packed channels” Journal of Thermo-physics and Heat Transfer, 13 **(1999)** 517-521.

Rady, M.: “Granular phase change materials for thermal energy storage: Experiments and numerical simulations”, Applied Thermal Engineering, 29 **(2009)** 3149-3159

Rimkevicius, S.: Vilemas, J.: Uspuras, E.: “Thermal hydraulic characteristics in annular pebble beds with axial and radial gas flows”, Experimental Heat Transfer, 20 **(2007)** 185-196.

Testu, A.: Didierjean, S.: Maillet, D.: Moyne, C.: Metzger, T.: Niass, T.: “Thermal dispersion for water or air flow through a bed of glass beads”, International Journal of Heat and Mass Transfer, 50 **(2007)** 1469-1484.

Vande Wouwer, A.: Point, N.: Porteman, S.: Remy, M.: “An approach to the selection of optimal sensor locations in distributed parameter systems” Journal of Process Control, 10 **(2000)** 291-300.

Wakao, N.: “Effect of fluid dispersion coefficient on particle-to-fluid heat transfer coefficients in packed beds: Correlation of Nusselt numbers” Chemical Engineering Science, 34 **(1979)** 325-336.

Wakao, N.: Kaguei, S.: Shen, J.: “Measurements of particle-to-gas heat transfer coefficients from one-shot thermal responses in packed beds” Chemical Engineering Science, 36 **(1981)** 1283-1286.

Wen, D.: Ding, Y.: “Heat transfer of gas flowing through a packed bed” Chemical Engineering Science, 61 **(2006)** 3532-3542.

# APPENDIX A

**ONE DIMENSIONAL HEAT TRANSFER EQUATION**

Consider the one dimensional heat transfer system which is shown in Figure III.1. If the system is in a steady state then the problem is a simple one and it is only needed to integrate Equation (II.2) and substitute the appropriate values to solve for the desired quantity. However, if the temperature of the solid is changing with time, or if there are heat sources or sinks within the solid, the situation is more complex. We consider the general case where the temperature may be changing with time and heat sources may be present within the body (Holman, 1983). For the element of thickness *dx* and control volume, the following balances can be made:

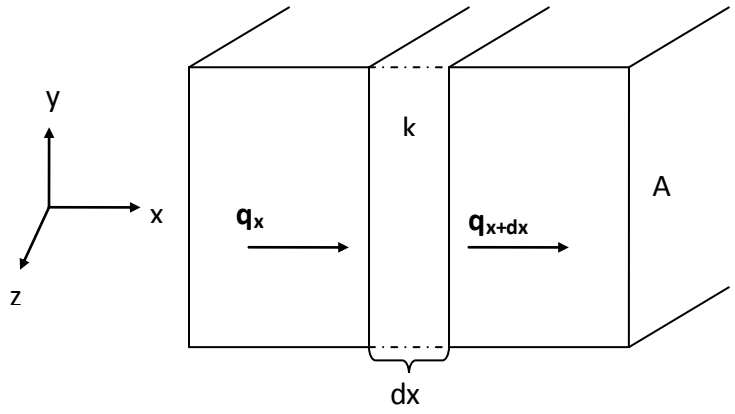


**Appendix A-Figure 1 Elemental volume for one dimensional heat conduction analysis**

- Direction of the heat is at the way of decreasing temperature.
- The rate of heat flow is proportional with the heat flowing area and the temperature profile perpendicular to this area.
- Gained or lost heat of a material due to temperature raise or fall is related to temperature difference and mass of material.

It is needed to derive an energy equation for any finite material with the control volume of;

$$\Delta V = \Delta x.\Delta y.\Delta z \qquad (A.1)$$

where

$\Delta x$ : Thickness in the x direction (m)

$\Delta y$ : Thickness in the y direction (m)

$\Delta z$ : Thickness in the z direction (m)

If $\rho_s$ is constant, the mass of this volume will be equal to;

$$\Delta M = \rho_s \Delta x \Delta y \Delta z \qquad (A.2)$$

where,

$\rho_s$ : Density of the solid control volume (kg/m$^3$)

Heat conduction through the *x* direction is related to temperature gradient at the same direction as shown in Equation II.2.

For a time of $\Delta t$, the conducted heat through the area A at the position of x is;

$$\Delta q_x = -k.\frac{\partial T}{\partial x}|\Delta y \Delta z \Delta t \qquad (A.3)$$

Same as above, for a time of $\Delta t$, the conducted heat through the area of A at the position of x + $\Delta$x is;

$$\Delta q_{x+\Delta x} = -k.\frac{\partial T}{\partial x}|\Delta y \Delta z \Delta t \qquad (A.4)$$

Then the heat absorbed by the material in time of $\Delta t$ is;

$$\Delta q_x - \Delta q_{x+\Delta x} = \Delta(mCT) \qquad (A.5)$$

where,

*m* : The mass of the control volume (kg)

*C* : Heat capacity of the solid (J/kg$^o$C)

At any point (*x*) and any time (*t*) the amount of heat produced is given as a function of *f(x,y,z,t)*

$$\Delta q^{l} = f(x, y, z, t)\Delta x \Delta y \Delta z \Delta t \qquad (A.6)$$

Basically, a heat transfer phenomena can be written as;

$$input - output + production = accumulation$$

$$\overbrace{\left[-k\frac{\partial T}{\partial x}|\Delta y\Delta z\Delta t\right]}^{\text{input at x}} - \overbrace{\left[-k\frac{\partial T}{\partial x}|\Delta y\Delta z\Delta t\right]}^{\text{output at x+}\Delta x} + \overbrace{f(x,y,z,t)}^{\text{production}}\overbrace{\Delta x\Delta y\Delta z\Delta t} = \overbrace{(\rho C\Delta T\Delta x\Delta y\Delta z)}^{\text{accumulation}} \quad (A.7)$$

Dividing the equation with *"(Δx.Δy.Δz.Δt)"* and taking limit when $\Delta x$ and $\Delta t$ approach to zero gives the one dimensional heat equation.

$$\frac{\partial}{\partial x}\left(k.\frac{\partial T}{\partial x}\right) + f(x,y,z,t) = \rho_s C\frac{\partial T}{\partial t} \quad (A.8)$$

Neglecting the heat production is convenient for the present study. Finally, the one dimensional heat equation (Eq. A.9) is obtained.

$$\frac{\partial}{\partial x}\left(k.\frac{\partial T}{\partial x}\right) = \rho_s C\frac{\partial T}{\partial t} \quad (A.9)$$

# APPENDIX B

**NUMERICAL SOLUTION FOR ONE DIMENSIONAL HEAT TRANSFER EQUATION**

Finite difference method is used for the numerical solution of the present mathematical model throughout all the steps of this study (Karahan, 2008).

**Finite difference method**

$$k\frac{\partial^2 T}{\partial x^2} = \frac{\partial T}{\partial t} \qquad (B.1)$$

The above equation is similar to the one dimensional heat transfer equation. The equation can be solved by explicit or implicit method.

In the present study, the explicit method is used to solve the one dimensional heat transfer equation, numerically.

The first term of the equation can be solved by central finite difference approach;

$$\frac{\partial^2 T}{\partial x^2} = \frac{T_{i+l}^{l} - 2T_i^l + T_{i-l}^{l}}{\Delta x^2} \qquad (B.2)$$

*Note:* This equation has an error of, $\theta[(\Delta x)^2]$. The notation of "*ı*" refers time.

For the second term, forward finite difference approach can be used;

$$\frac{\partial \mathrm{T}}{\partial \mathrm{t}} = \frac{\mathrm{T_i^{l+1}} - \mathrm{T_i^l}}{\Delta \mathrm{t}} \qquad (B.3)$$

***Note:*** This equation has an error of, $\theta[(\Delta t)]$.

If these two equations are replaced on the original equation, we have;

$$\mathrm{k}.\frac{\mathrm{T_{i+l}^l} - 2\mathrm{T_i^l} + \mathrm{T_{i-l}^l}}{\Delta \mathrm{x}^2} = \frac{\mathrm{T_i^{l+1}} - \mathrm{T_i^l}}{\Delta \mathrm{t}} \qquad (B.4)$$

Rewriting the Eq. (B.4) gives;

$$T_i^{l+1} = T_i^l + \lambda.(T_{i+1}^l - 2T_i^l + T_{i-1}^l) \quad (B.5)$$

Where $\lambda = k.\Delta t/(\Delta x)^2$

At this point, investigation of the given below figure may help to understand the numerical approach.

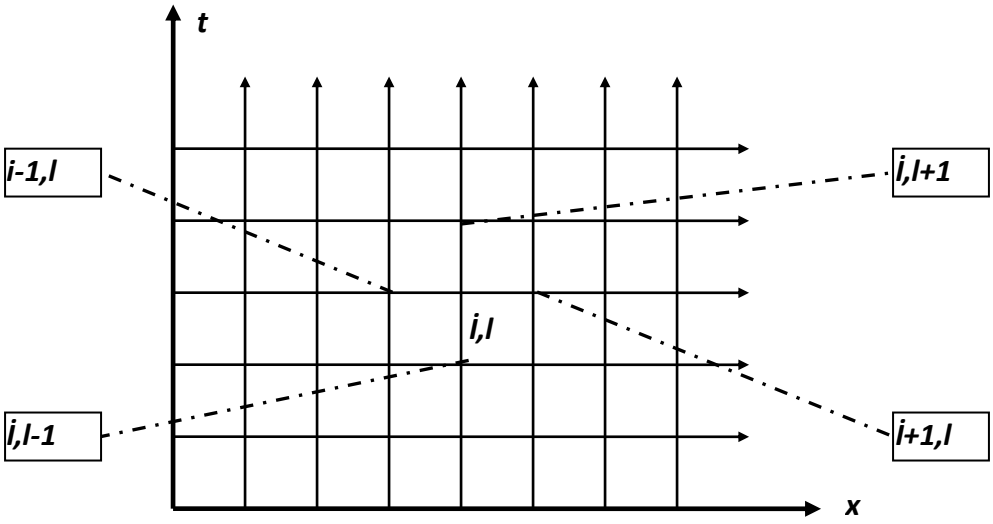


**Appendix B-Figure 1 Schematic image of numerical solution approach**

$$T_0^{l+1} = T_0^l + \lambda.(T_1^l - 2T_0^l + T_{-1}^l) \quad (B.6)$$

**GENERAL NUMERICAL STRUCTURE USED IN ALL SIMULATIONS**

The numerical structure used in all of the simulation in the present study is based on the above finite difference method. All of the numerical equations are given below.

$$T(i,j) = T(i,j-1) + K\big(-T(i,j-1) + T(i-1,j-1)\big) - L\big(T(i,j-1) - T(i-1,j-1)\big) - M\big(T(i,j-1) - T_s(i,j-1)\big) - U(T(i,j-1) - T_{air}) \quad (B.7)$$

$$T_s(i,j) = T_s(i,j-1) + P\big(T(i,j-1) - T_s(i,j-1)\big) \quad (B.8)$$

# APPENDIX C

## TWO-DIMENSIONAL HEAT TRANSFER

Unlike one-dimensional heat transfer equation, two-dimensional heat transfer equation includes heat transfer mechanism along the radial direction of a cylindrical control volume. It can be said that two dimensional heat transfer equation is an advanced version of one-dimensional heat transfer equation. The equation is based on the cylindrical control volume which is shown in Figure C.1.

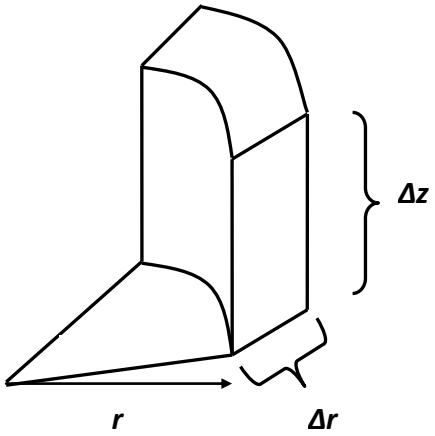


**Appendix C-Figure 1 Differential control volume in cylindrical coordinates**

Overall control volume calculation of the above cylindrical volume is given below.

$$\Delta V = r.\Delta\theta.\Delta r.\Delta z$$

## ENERGY BALANCE FOR THE CONTROL VOLUME

Using heat flow areas for the heat flow directions given in Table C.1, an energy balance is derived in Eq. C.1 for the cylindrical control volume.

**Appendix C-Table 1 Directions and heat flow area for differential control volume**

| Direction | Heat flow area |
|---|---|
| r | $r.\Delta\theta.\Delta z$ |
| $\theta$ | $\Delta r.\Delta z$ |
| z | $r.\Delta\theta.\Delta r$ |

$$\overbrace{\left[-k\frac{\partial T}{\partial r}r\Delta\theta\Delta z\Delta t\right]_{r}^{at}-\left[-k\frac{\partial T}{\partial r}r\Delta\theta\Delta z\Delta t\right]_{r+\Delta r}^{at}}^{\text{1. term}}$$
$$+\overbrace{\left[-k\frac{\partial T}{\partial z}r\Delta\theta\Delta r\Delta t\right]_{z}^{at}-\left[-k\frac{\partial T}{\partial z}r\Delta\theta\Delta r\Delta t\right]_{z+\Delta z}^{at}}^{\text{2. term}}$$
$$+\overbrace{\left[\rho C_p V_z T r\Delta\theta\Delta r\Delta t\right]_{z}^{at}-\left[\rho C_p V_z T r\Delta\theta\Delta r\Delta t\right]_{z+\Delta z}^{at}}^{\text{3. term}}$$
$$-\overbrace{\left[ha(T-T_s)r\Delta\theta\Delta r\Delta z\Delta t\right]}^{\text{4. term}}$$
$$+\overbrace{\left[\rho C_p T.r\Delta\theta\Delta r\Delta z\right]_{t}^{at}-\left[\rho C_p T.r\Delta\theta\Delta r\Delta z\right]_{t+\Delta t}^{at}}^{\text{5. term}}=0 \qquad (C.1)$$

The first term of the above equation represents heat transfer by conduction into the control volume during a time period of $\Delta t$. For the first term of the energy balance, the heat conduction at r direction is considered during $\Delta t$.

The second term of the above equation represents heat transfer by conduction into the control volume during a time period of $\Delta t$. For the second term of the energy balance, the heat conduction at z direction is considered during $\Delta t$.

The third term of the above equation represents heat flow due to bulk flow with a velocity of $V_z$ during a time period of $\Delta t$. The heat flow due to bulk flow occurs at z direction.

The forth term of the energy balance represents heat transfer between the fluid and solid particles by convection during a time period of $\Delta t$.

The last term of the balance equations represents heat content of the control volume during a time period of $\Delta t$.

Here, the above energy balance equation is divided by $\Delta r.\Delta\theta.\Delta z.\Delta t$ and limit of the equation is taken as $\Delta r$, $\Delta\theta$, $\Delta z$, $\Delta t$ approach zero.

$$\lim_{\Delta r\to 0}\frac{\left(-rk\frac{\partial T}{\partial r}\right)_{r}^{at}-\left(-rk\frac{\partial T}{\partial r}\right)_{r+\Delta r}^{at}}{\Delta r}+\lim_{\Delta z\to 0}\frac{\left(-rk\frac{\partial T}{\partial z}\right)_{z}^{at}-\left(-rk\frac{\partial T}{\partial z}\right)_{z+\Delta z}^{at}}{\Delta z}$$
$$+\lim_{\Delta z\to 0}\frac{\left(r\rho C_p V_z T\right)_{z}^{at}-\left(r\rho C_p V_z T\right)_{z+\Delta z}^{at}}{\Delta z}-rha(T-T_s)$$
$$+\lim_{\Delta t\to 0}\frac{\left(r\rho C_p T\right)_{t}^{at}-\left(r\rho C_p T\right)_{t+\Delta t}^{at}}{\Delta t}=0 \qquad (C.2)$$

The equation can be written as below;

$$\frac{\partial}{\partial r}\left(rk\frac{\partial T}{\partial r}\right)+\frac{\partial}{\partial z}\left(rk\frac{\partial T}{\partial z}\right)-\varepsilon\frac{\partial\left(r\rho C_p V_z T\right)}{\partial z}-rha(T-T_s)-\varepsilon\frac{\partial\left(r\rho C_p T\right)}{\partial t}=0 \qquad (C.3)$$

Rewriting the equation gives;

$$\frac{\partial}{\partial r}\left(rk\frac{\partial T}{\partial r}\right)+r\frac{\partial}{\partial z}\left(k\frac{\partial T}{\partial z}\right)-\varepsilon r\frac{\partial\left(\rho C_p V_z T\right)}{\partial z}-rha(T-T_s)-\varepsilon r\frac{\partial\left(\rho C_p T\right)}{\partial t}=0 \qquad (C.4)$$

Dividing the whole equation by r, gives;

$$\varepsilon\frac{\partial\left(\rho C_p T\right)}{\partial t}=\frac{1}{r}\frac{\partial}{\partial r}\left(rk\frac{\partial T}{\partial r}\right)+\frac{\partial}{\partial z}\left(k\frac{\partial T}{\partial z}\right)-\varepsilon\frac{\partial\left(\rho C_p V_z T\right)}{\partial z}-ha(T-T_s)-Ua_t(T-T_{air}) \qquad (C.5)$$

***Boundary conditions for the last equation:***

1.

$$\text{at } z=0\ ;T=T_{in}$$

Where, $T_{in}$ represents the temperature of the fluid at the inlet point.

2.

$$\text{at } z=L\ ;\frac{\partial T}{\partial z}=0$$

Where, heat transfer reaches zero at L due to no change in temperature at z direction.

3.

$$at\ r = 0\ ;\ \frac{\partial T}{\partial r} = 0$$

The third boundary condition represents no temperature change at the centre of the cylinder. It is also called symmetry boundary condition or min-max boundary condition.

4.

$$at\ r = R\ ;\ -k_t \frac{\partial T}{\partial r} = U.A.(T(R) - T_s)$$

Where, $k_t$ is thermal conduction of the heat storage unit, and T(R) is outside temperature of heat storage unit, and $T_s$ is surrounding air temperature.

Finally the initial condition is given as;

$$at\ t = 0\ ; T = T_0$$

# APPENDIX D

## D.1 WATER PROPERTIES

Table 1 shows the properties of the water the temperatures. Using this table it is possible to derive the equations which represent the behavior of the parameters with changing temperature (Geankoplis, 2007).

**Appendix D-Table 1 Water Properties**

| *T °C* | *Density ρ kg/m³* | *Dynamic viscosity μ cp* | *Kinematic viscosity, v m²/s* | *Expansion Coefficient 1/°C* | *$C_f$ kj/kg°C* | *Pr* |
|---|---|---|---|---|---|---|
| 0.01 | *999.8* | 1.78 | $1.792x10^{-6}$ | $-0.07x10^{-3}$ | *4.210* | 13.67 |
| 5 | *1000* | 1.52 | | $0.160\,x10^{-3}$ | *4.204* | |
| 10 | *999.8* | 1.31 | $1.304\,x10^{-6}$ | $0.088\,x10^{-3}$ | *4.193* | 9.47 |
| 15 | *999.2* | 1.14 | | $0.151\,x10^{-3}$ | *4.186* | |
| 20 | *998.3* | 1.00 | $1.004\,x10^{-6}$ | $0.207\,x10^{-3}$ | *4.183* | 7.01 |
| 25 | *997.1* | 0.890 | | $0.257\,x10^{-3}$ | *4.181* | |
| 30 | *995.7* | 0.798 | $0.801\,x10^{-6}$ | $0.303\,x10^{-3}$ | *4.179* | 5.43 |
| 35 | *994.1* | 0.719 | | $0.345\,x10^{-3}$ | *4.178* | |
| 40 | *992.3* | 0.653 | $0.658\,x10^{-6}$ | $0.385\,x10^{-3}$ | *4.179* | 4.34 |
| 45 | *990.2* | 0.596 | | $0,420\,x10^{-3}$ | *4.181* | |
| 50 | *988* | 0.547 | $0.553\,x10^{-6}$ | $0.457\,x10^{-3}$ | *4.182* | 3.56 |
| 55 | *986* | 0.504 | | $0.486\,x10^{-3}$ | *4.183* | |
| 60 | *983* | 0.467 | $0.474\,x10^{-6}$ | $0.523\,x10^{-3}$ | *4.185* | 2.99 |
| 65 | *980* | 0.434 | | $0.544\,x10^{-3}$ | *4.188* | |
| 70 | *978* | 0.404 | $0.413\,x10^{-6}$ | $0.585\,x10^{-3}$ | *4.191* | 2.56 |

## D.2 CALCULATION OF MODEL PARAMETERS

Almost every model parameter is a function of temperature. Therefore it is needed to shown how these parameters are changing with temperature. Also, derivation of the constant parameters is indicated in the following pages. These derivations were obtained using curve fitting method by the software Microsoft Excel®.

### D.2.1 Calculation of Fluid Density

Figure 1 represents the changing of the fluid density with temperature. The effect of the temperature changes on the fluid density is applied to the mathematical model by using the Eq. (D.1) which represents the behavior of the fluid density at different temperatures.

$$\rho = -1 \times 10^{-6} T^3 - 0.0031 T^2 - 0.0112 T + 999.41 \qquad \text{(D.I)}$$

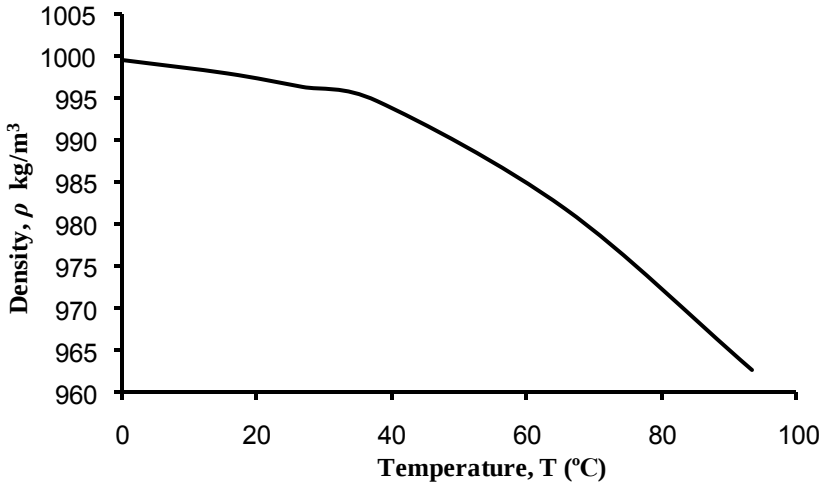


**Appendix D-Figure 1 Changing of the fluid density with temperature**

### D.2.2 Calculation of Fluid Viscosity

Figure 2 represents the changing of the fluid viscosity with temperature. The effect of the temperature changes on the fluid viscosity is applied to the mathematical model by using the Eq. (D.2) which represents the behavior of the fluid viscosity at different temperatures.

$$\mu = -3 \times 10^{-9} T^3 + 6 \times 10^{-7} T^2 - 5 \times 10^{-5} T + 0.0018 \qquad \text{(D.2)}$$

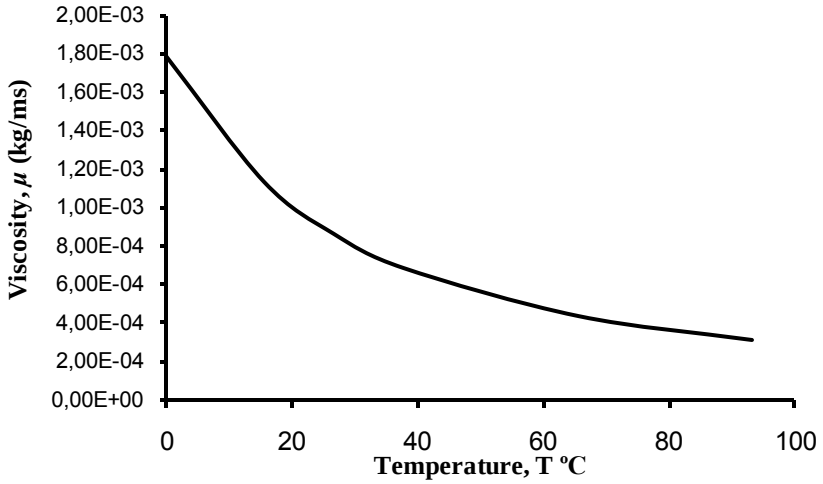


**Appendix D-Figure 2 Changing of the fluid viscosity with temperature**

### D.2.3 Calculation of Heat Capacity

Figure 3 represents the changing of heat capacity of the fluid with temperature. The effect of the temperature changes on heat capacity of the fluid is applied to the mathematical model by using the Eq. (D.3) which represents the behavior of the heat capacity of the fluid at different temperatures.

$$C_f = 1 \times 10^{-8} T^4 - 2 \times 10^{-6} T^3 + 0.0002 T^2 - 0.0047 T + 4.2289 \qquad (D.3)$$

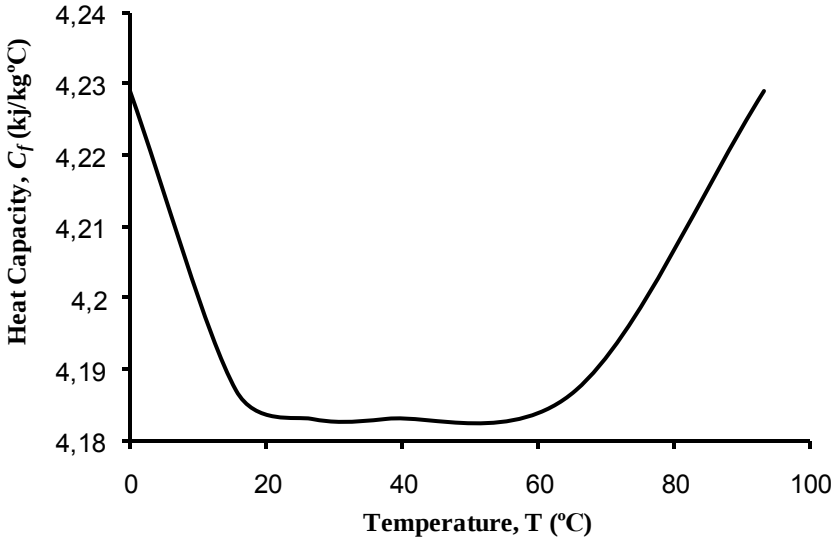


**Appendix D-Figure 3 Changing of heat capacity of the fluid with temperature**

### D.2.4 Calculation of Heat Conduction Coefficient

Figure 4 represents the changing of heat conduction coefficient of the fluid with temperature. The effect of the temperature changes on heat conduction coefficient of the fluid is applied to the mathematical model by using the Eq. (D.4) which represents the behavior of heat conduction coefficient of the fluid at different temperatures.

$$k = 1 \times 10^{-7}T^3 + 9 \times 10^{-6}T^2 + 0.0014T + 0.5684 \qquad (D.4)$$

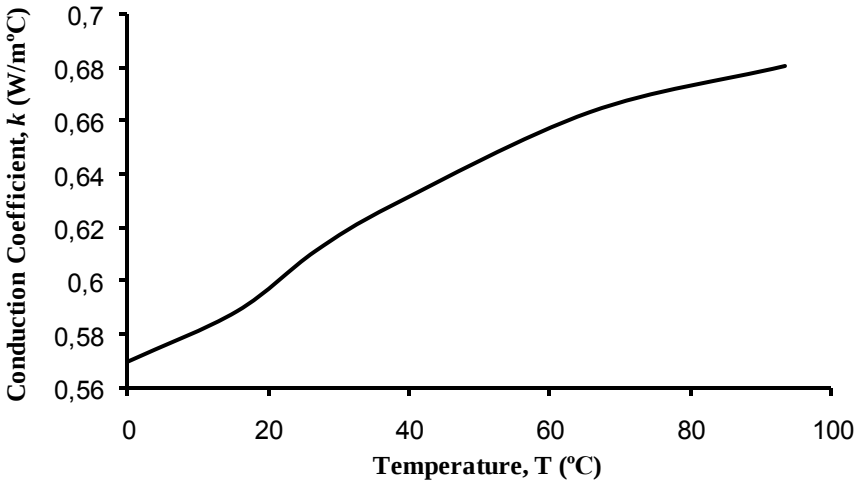


**Appendix D-Figure 4 Changing of heat conduction coefficient of the fluid with temperature**

### D.2.5 Calculation of Convective Heat Transfer Coefficient, *h*

Convection coefficient of water changes with temperature and flow rate. The relation between ***h*** and ***Nu*** is given in Chapter II. AS it can be seen in Eq. D.5 the correlation of Hanrattry (1954) includes *Re* and *Pr* numbers and void fraction ε. The relation between convective heat transfer coefficient and flow rate is hidden in Re number.

$$Nu = \frac{1.1}{\varepsilon^{1/2}}[6(1-\varepsilon)]^{1/2}Re^{1/2}Pr^{1/2} \qquad (D.5)$$

The dependence of h to Nu number is given in Eq. D.6.

$$Nu = \frac{hD_p}{k} \qquad (D.6)$$

### D.2.6 Calculation of Fluid Velocity $V_z$

The water flows through the glass beads has different flow rates at different experiments. Thus, fluid velocity values must be calculated to be used in the present mathematical model. Considering the void fraction and fluid flowing area across the bed the Eq. D.7 gives the fluid velocity for different flow rates.

$$V_z = \frac{\dot{V}}{A\varepsilon} \ {}^{m}/_{S} \tag{D.7}$$

### D.2.7 Calculation of Overall Heat Transfer Coefficient *U*

The direction of heat flow along the entire system is from the fluid to the environment of the system. The heat transfers from the fluid to the tank by convection, then transfers to the other side of the tank wall by conduction and then transfers to the surrounding air by convection. Considering these steps of heat transfer mechanisms in the system, the Eq. D.8 is written.

$$\frac{1}{U} = \frac{1}{h} + \frac{\Delta x_{tank}}{k_{tank}} + \frac{1}{h_{air}} \tag{D.8}$$

In Eq. D.8 thermal conductivity of the tank, $k_{tank}$ and convective heat transfer coefficient of air, $h_{air}$ are assumed constant.

### D.2.8 Calculation of Specific Heat Transfer Surface "$a_t$"

The heat transfer area for the unit volume of the tank is represented by the term "$a_t$".

$$a_t = \frac{overall\ surface\ area\ of\ empty\ tank}{overall\ volume\ of\ empty\ tank} \ {}^{m^2}/_{m^3} \tag{D.9}$$

To be able to calculate the overall surface area of the tank, areas of cylindrical wall, bottom and top has to be known. The calculation of overall surface area of empty tank is shown by the equations below.

$$S_{wall} = \pi D_t H_t = \pi(0.223) \times (0.235) = 0.165 \ m^2 \tag{D.10}$$

$$S_{bottom} = S_{top} = \frac{\pi D_t^2}{4} = \frac{\pi(0.223)^2}{4} = 0.039\ m^2 \quad (D.11)$$

$$S_{overall} = 0.165 + 2 \times 0.039 = 0.243\ m^2 \quad (D.12)$$

$$a_t = \frac{S_{overall}}{V_{tank}} = \frac{0.243\ m^2}{0.00917\ m^3} = 26.5\ {}^{m^2}/_{m^3} \quad (D.13)$$

### D.2.9 Calculation of Specific Surface Area of Glass Beads *"a"*

Surface areas of glass beads are differ across the bed. The packed bed system of the present study satisfies the poured random packing conditions. The relation between the particle diameter and the term "a" is given in Eq. D.14.

$$a = 6\frac{(1-\varepsilon)}{D_p}\ {}^{m^2}/_{m^3} \quad (D.14)$$

## D.3 CALCULATION OF DIMENSIONLESS VARIABLES AND GROUPS

### D.3.1 Dimensionless Temperature and Time

Calculation of dimensionless temperature **θ** is given in Eq. (D.15).

$$\theta = \frac{T(t) - T_\infty}{T_0 - T_\infty} \quad (D.15)$$

Calculation of dimensionless time **τ** is given Eq. (D.16).

$$\tau = \frac{\dot{V}t}{\varepsilon V} \quad (D.16)$$

### D.3.2 Dimensionless Groups and their physical meanings

Calculation of dimensionless groups that is used in this study is given below equations.

**Calculation of Reynolds Number, Re**

Reynolds number is a measure of the ratio of kinetic forces to viscous forces. Consequently quantifies the relative importance of these two types of forces for given flow conditions.

$$Re = \frac{\rho_f D_p V_z}{\varepsilon \mu} \tag{D.17}$$

**Calculation of Prandtl Number, Pr**

The physical meaning of Prandtl number can be described as the ratio of momentum diffusivity (kinematic viscosity) to thermal diffusivity.

$$Pr = \frac{C_f \mu}{k} \tag{D.18}$$

**Calculation of Peclet Number, Pe**

The physical meaning of Peclet number can be described as the ratio of the rate of advection of a physical quantity by the flow to the rate of diffusion of the same quantity driven by an appropriate gradient.

$$Pe = RePr \tag{D.19}$$

**Calculation of Rayleigh Number, Ra**

The physical meaning of Rayleigh number can be viewed as the ratio of buoyancy forces and (the product of) thermal and momentum diffusivities.

$$Ra = \frac{g\beta K \Delta T D_{tank}}{\upsilon \alpha_m} \tag{D.20}$$

$g$ : Gravity ($m/s^2$)

$\beta$ : The thermal expansion coefficient (1/ºC)

$K$ : Permeability of the packed bed ($(\varepsilon^3 D_p^2)/(180(1-\varepsilon)^2)$)

$\upsilon$ : Kinematic viscosity of fluid ($m^2/s$)

$\alpha_m$ : Media thermal diffusivity ($\alpha_m = k/(\rho C_f)$)

**Calculation of Nusselt Number, Nu**

If *Nu*=1, this means that the convection and conduction terms have relatively similar magnitude and thus it is characterized by the laminar flow. On the other hand, large *Nu* implies that the convective term is dominant, which typically characterized by turbulent flows.

$$Nu = \frac{h_f D_p}{k} = \frac{convective\ heat\ transfer}{conductive\ heat\ transfer} \qquad (D.21)$$

$h_f$ : Convective heat transfer coefficient of the fluid (J/m$^2$ s ºC)

$D_p$ : Particle diameter (m)

$k$ : Thermal conductivity of fluid (J/m s ºC)

# APPENDIX E

**FURTHER MODEL RESULTS**

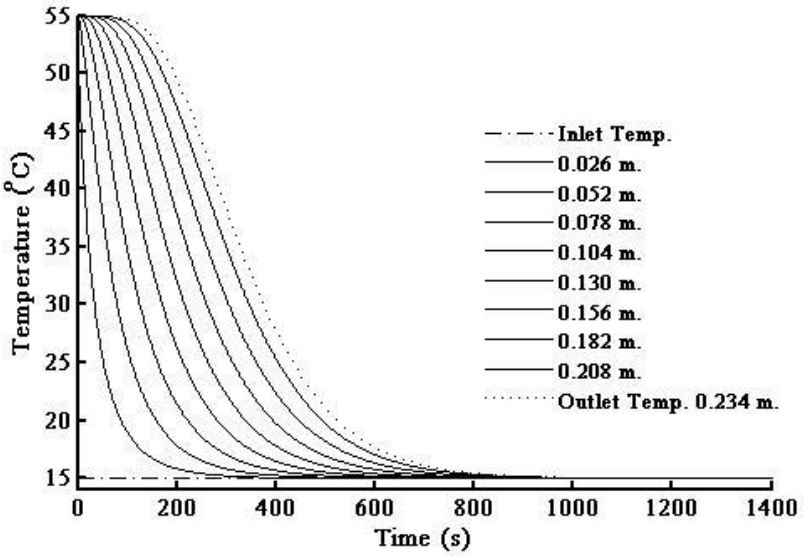


**Appendix E- Figure 1 Temperature profiles across the packed bed for the simulation of a cooling experiment (Re=25.2, Flow rate=0.0166 L/s, $T_{in}$=15°C)**

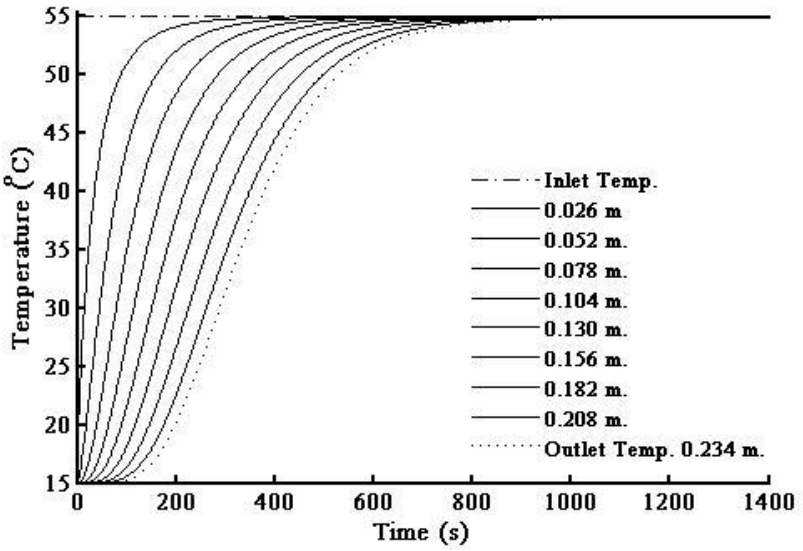


**Appendix E- Figure 2 Temperature profiles across the packed bed for the simulation of a heating experiment (Re=56.1, Flow rate=0.0166 L/s, $T_{in}$=55°C)**

## FURTHER MODEL AND EXPERIMENTAL RESULTS

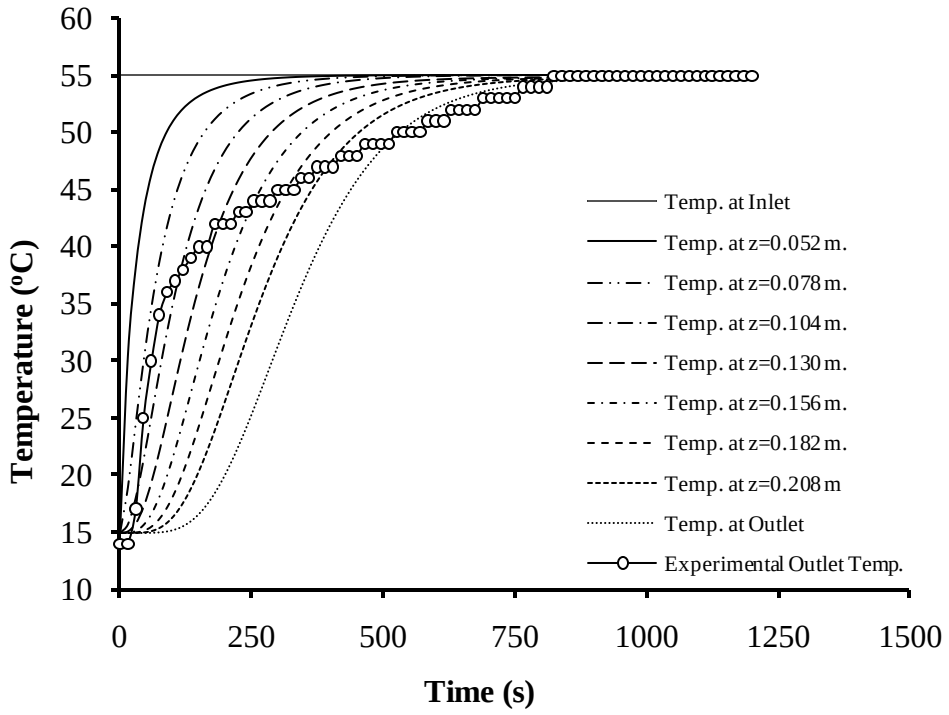


**Appendix E- Figure 3 Temperature profiles across the packed bed for the simulation of a heating experiment together with heating experimental results (Re=56.1, Flow rate=0.0166 L/s, $T_{in}$=55ºC)**

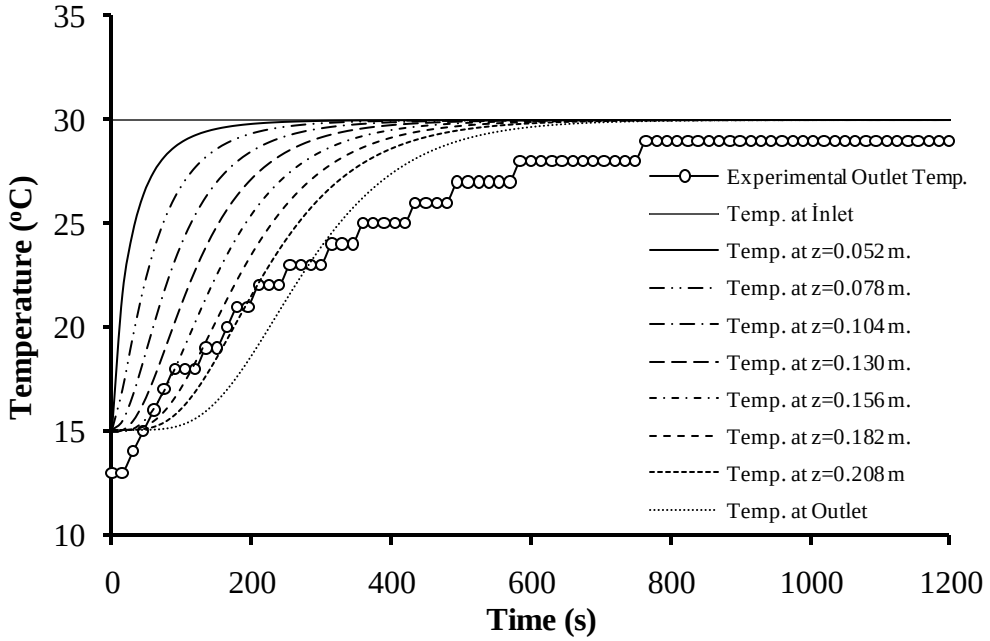


**Appendix E- Figure 4 Temperature profiles across the packed bed for the simulation of a heating experiment together with heating experimental results (Re=51.2, Flow rate=0.0227 L/s, $T_{in}$=30ºC)**

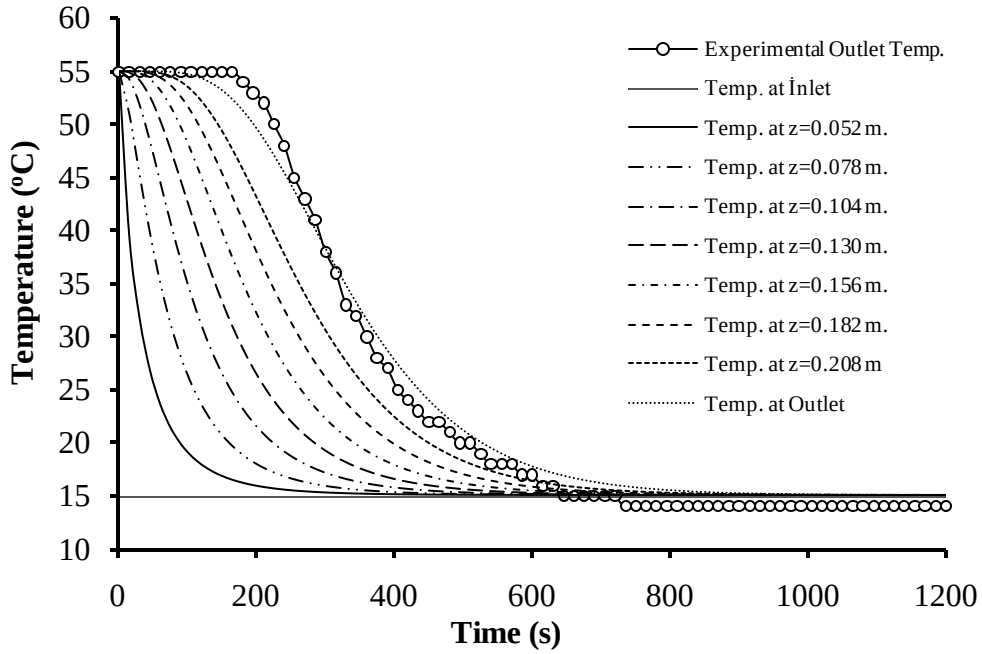


**Appendix E- Figure 5 Temperature profiles across the packed bed for the simulation of a cooling experiment together with cooling experimental results (Re=25.2, Flow rate=0.0166 L/s, $T_{in}$=15ºC)**

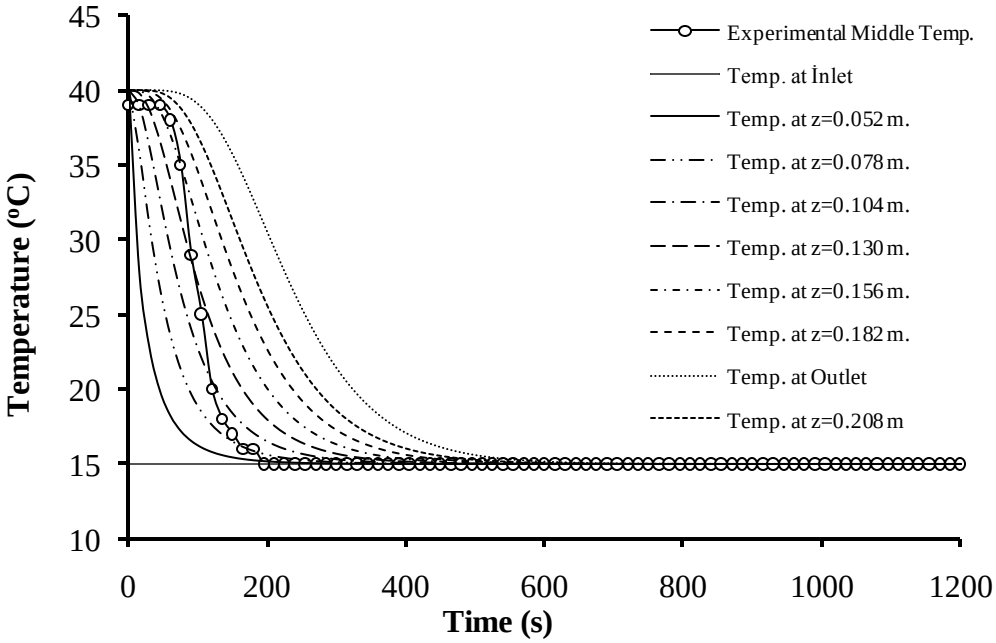


**Appendix E- Figure 6 Temperature profiles across the packed bed for the simulation of a cooling experiment together with cooling experimental results (Re=33.2, Flow rate=0.0202 L/s, $T_{in}$=15ºC)**

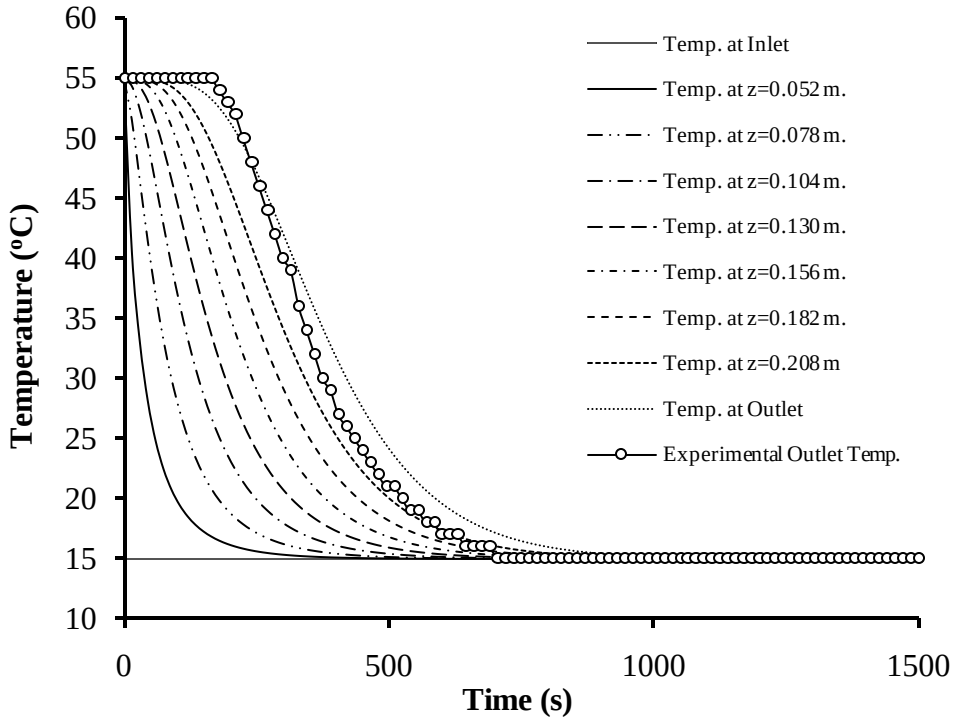


**Appendix E- Figure 7 Temperature profiles across the packed bed for the simulation of a cooling experiment together with cooling experimental results (Re=22.4, Flow rate=0.0148 L/s, $T_{in}$=15ºC)**

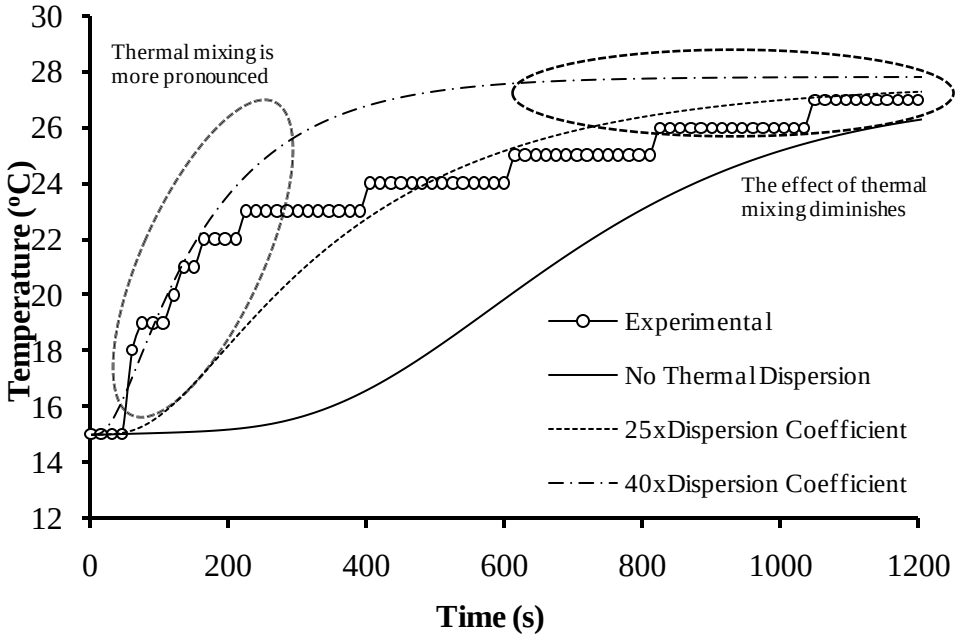


**Appendix E- Figure 8 Thermal mixing effects**

# AUTOBIOGRAPHY

*I was born in Üsküdar on 29th of February in 1984. My father is a retired worker and my mother is a housewife. I have two elder sisters and brothers, all married.*

*I am graduated from a primary school Kılıçarslan İ.Ö.O. in Pendik, İstanbul, where I grow up and I am still residing. Then, I graduated from high school, Pendik Lisesi (foreign language based school). In 2005, I had been transferred from Atatürk University to Marmara University at the end of my freshman year in Erzurum. After accomplishing my Bachelor's Degree in Chemical Engineering, I have been admitted for Master Programme at Marmara University in 2009.*

*Following my graduation at the end of this academic year, I will join Turkish Armed Forces to fulfill my military duty. Eventually, my desire and aim is to carry out my profession as a chemical engineer at public utilities or universities.*

**July 2011**

**Osman ÖZDEMİR**